Paradoxical enhancement of chemoreceptor detection sensitivity by a sensory adaptation enzyme

Run-Zhi Lai (赖润智)[a], Xue-Sheng Han[a], Frederick W. Dahlquist[b], and John S. Parkinson[a,1]

[a]Biology Department, University of Utah, Salt Lake City, UT 84112; and [b]Department of Chemistry and Biochemistry, University of California, Santa Barbara, CA 93106

Edited by Susan S. Golden, University of California, San Diego, La Jolla, CA, and approved July 27, 2017 (received for review May 31, 2017)

A sensory adaptation system that tunes chemoreceptor sensitivity enables motile *Escherichia coli* cells to track chemical gradients with high sensitivity over a wide dynamic range. Sensory adaptation involves feedback control of covalent receptor modifications by two enzymes: CheR, a methyltransferase, and CheB, a methylesterase. This study describes a CheR function that opposes the signaling consequences of its catalytic activity. In the presence of CheR, a variety of mutant serine chemoreceptors displayed up to 40-fold enhanced detection sensitivity to chemoeffector stimuli. This response enhancement effect did not require the known catalytic activity of CheR, but did involve a binding interaction between CheR and receptor molecules. Response enhancement was maximal at low CheR:receptor stoichiometry and quantitative analyses argued against a reversible binding interaction that simply shifts the ON–OFF equilibrium of receptor signaling complexes. Rather, a short-lived CheR binding interaction appears to promote a long-lasting change in receptor molecules, either a covalent modification or conformation that enhances their response to attractant ligands.

bacterial chemotaxis | receptor methyltransferase | dynamic-bundle model | signaling conformation | nonequilibrium mechanism

Motile bacteria, despite their small size and simple cellular architecture, track chemical gradients in their living environments with extraordinary precision (see refs. 1 and 2 for reviews). They do so with only a handful of different proteins organized in a sensory signaling network that has stimulus integration, amplification, and memory capabilities. The extensively studied chemotaxis machinery of *Escherichia coli* has provided the molecular paradigm for transmembrane and intracellular signaling mechanisms in microbial chemosensory systems. This report describes a long-unrecognized activity of a central component of the *E. coli* chemotaxis machinery, suggesting that there are important new molecular lessons to learn from this structurally simple, yet functionally sophisticated, signaling system.

E. coli senses attractant and repellent chemicals with transmembrane chemoreceptors known as methyl-accepting chemotaxis proteins (MCPs) (3). MCPs form networked arrays of signaling complexes, typically at the cell poles, that produce highly sensitive and cooperative responses to small chemoeffector concentration changes. The four MCPs of *E. coli* (Tsr, Tar, Tap, and Trg) have a common functional architecture comprising a periplasmic sensing domain and a cytoplasmic signaling domain (Fig. 1). An interposed HAMP domain communicates conformational changes between the sensing and signaling domains through an extended four-helix coiled-coil that contains sites for sensory adaptation adjustments of receptor signal output (4). The chemoreceptors modulate the activity of a histidine autokinase (CheA), which is stably coupled to receptors by a scaffolding protein (CheW). CheA donates its phosphoryl groups to CheY, a response regulator that in its phosphorylated form interacts with the basal bodies of the cell's flagellar motors to regulate their rotational behavior, producing locomotor responses. Phospho-CheY is short-lived, due to action of a dedicated phosphatase (CheZ), ensuring rapid swimming responses to chemoreceptor-triggered changes in CheA activity.

The gradient-tracking behavior of *E. coli* is made possible by a sensory adaptation system similar to those in many signal transduction systems of higher organisms (5, 6). Receptor/CheW/CheA core complexes approximate two-state signaling devices, having a kinase-active (ON) state and a kinase-inactive (OFF) state. A change in ligand occupancy shifts the ON–OFF equilibrium to initiate a motor response. The adaptation system then introduces covalent changes at specific receptor residues to adjust coiled-coil packing interactions of the four-helix signaling bundle and restore the prestimulus ON–OFF equilibrium (7). The adapted receptor-modification state reflects the chemoeffector concentration that elicited the covalent change. Thus, sensory adaptation enables *E. coli* to follow spatial chemical gradients by making temporal comparisons of current chemoeffector levels to a short-term "memory" of the recent chemical past, recorded in the form of a receptor-modification state.

Two MCP-specific enzymes mediate sensory adaptation in *E. coli*, CheR, a methyltransferase that converts glutamyl (E) sites to glutamyl-methyl esters (Em), and CheB, a methylesterase that hydrolyzes Em sites to E sites (7). The homodimeric serine chemoreceptor (Tsr) contains five adaptation sites per subunit (8, 9), two of which are genetically encoded as glutaminyl (Q) residues, which mimic the signaling properties of Em sites (Fig. 1). CheB irreversibly deamidates such Q sites to E sites, creating two additional substrate sites for subsequent methylation and demethylation reactions. The relative activities of the opposing CheR and CheB enzymes govern the direction and extent of adaptational modifications. The system produces perfect adaptation over a wide range of chemoeffector concentrations through

Significance

***Escherichia coli* cells track chemical gradients with high sensitivity over a wide dynamic range, using a feedback-controlled sensory adaptation system. CheR, a receptor methyltransferase, is a key component of the adaptation system. We discovered that CheR can enhance the response sensitivity of chemoreceptor molecules, a role that opposes the known signaling consequences of its catalytic activity. This enhancement effect requires CheR-receptor binding interactions, but is quantitatively inconsistent with a simple equilibrium binding mechanism. Rather, CheR binding appears to promote a long-lasting conformational or covalent change that enhances the affinity of chemoreceptor molecules for their attractant ligands. The CheR response enhancement effect opens a new window on the functional architecture of chemoreceptor molecules and their interactions with sensory adaptation enzymes.**

Author contributions: R.-Z.L., X.-S.H., F.W.D., and J.S.P. designed research; R.-Z.L. and X.-S.H. performed research; R.-Z.L., X.-S.H., F.W.D., and J.S.P. analyzed data; and R.-Z.L., F.W.D., and J.S.P. wrote the paper.

The authors declare no conflict of interest.

This article is a PNAS Direct Submission.

[1]To whom correspondence should be addressed. Email: parkinson@biology.utah.edu.

This article contains supporting information online at www.pnas.org/lookup/suppl/doi:10.1073/pnas.1709075114/-/DCSupplemental.

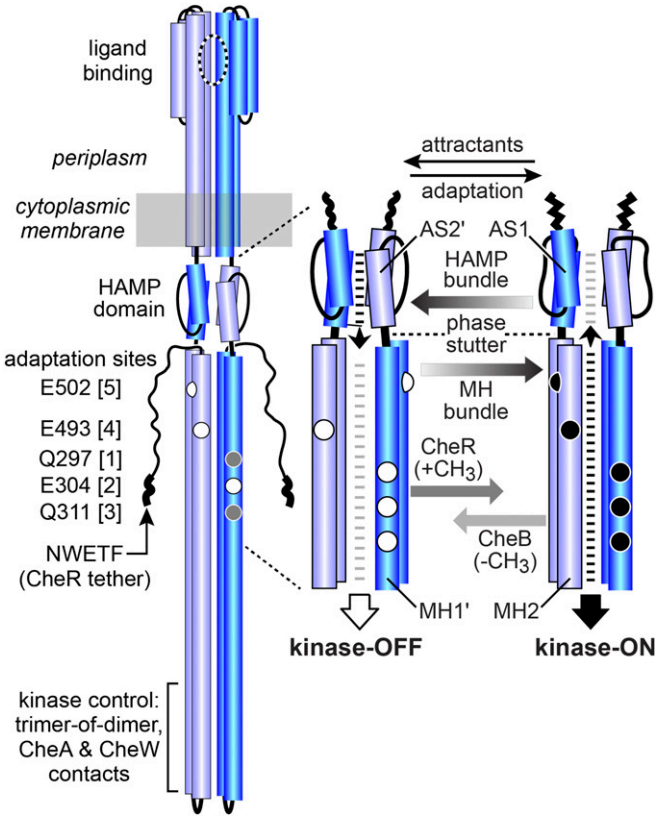

Fig. 1. Tsr structural elements for stimulus response and sensory adaptation. (*Left*) The Tsr molecule functions as a homodimer comprised of three subdomains. Cylindrical segments represent α-helices, drawn approximately to scale. Each subunit has five adaptation sites (only half are visible here): White circles represent E residues capable of accepting methyl groups; gray circles represent Q residues that must be deamidated by CheB before they can be methylated by CheR. The C terminus of each subunit bears a pentapeptide sequence (NWETF) that serves to tether CheR in the vicinity of the adaptation sites. (*Right*) Structural interactions between the HAMP and methylation helix (MH) bundles predicted by the dynamic-bundle model of HAMP signaling (18). The model assumes that chemoreceptors have two output signaling states (kinase-OFF; kinase-ON) but proposes that the ON–OFF equilibrium reflects shifts among multiple conformational states of the HAMP and MH bundles, whose packing stabilities are coupled in opposition by the phase stutter arrangement that joins their helices. Unmethylated adaptation sites (white circles) destabilize the MH bundle, allowing stronger HAMP packing. Methylated sites (black circles) stabilize the MH bundle, weakening HAMP packing. The HAMP–MH interplay poises the two bundles for stimulus responses: Attractants enhance HAMP stability to initiate a kinase-OFF output response; a subsequent methylation increase restores kinase-ON output during sensory adaptation. CheR preferentially acts on receptors in the OFF state; CheB preferentially acts on receptors in the ON state (1, 9). AS1 (shown) and AS1′ are the N-terminal HAMP helices; AS2 and AS2′ (shown) are the C-terminal HAMP helices. MH1 and MH1′ (shown) are the N-terminal helices of the methylation bundle; MH2 (shown) and MH2′ are the C-terminal helices of the methylation bundle.

integral feedback control (10–12): CheB operates preferentially on receptors in the ON state, shifting them toward OFF, whereas CheR operates preferentially on receptors in the OFF state, shifting them toward ON (Fig. 1).

The structural differences between ON-state and OFF-state receptors that define the CheB and CheR substrate preferences are not well understood. Adaptation site residues lie on solvent-exposed helix faces and share a consensus nine-residue motif at which CheR and CheB must bind for catalysis (13–15). Differences in higher-order structures of the methylation helix bundle presumably govern state-specific access to the substrate sites. Those structural differences probably involve changes in substrate helix stability and changes in the packing interactions between helices of the methylation bundle (9, 16–19).

The critical sensory adaptation roles of the CheR and CheB enzymes have been known for decades (20–25). Here, we report that CheR has a second function that opposes the signaling consequences of its catalytic activity. We show that binding interactions between CheR and the receptor methylation helices produce this effect, but the CheR methyltransferase reaction plays no part. Rather, CheR binding seems to produce a long-lasting structural change in receptor molecules, either a novel covalent modification or an altered native conformation that enhances their affinity for attractant ligands. The CheR response enhancement effect opens a new window on the functional architecture of chemoreceptor molecules and their interactions with sensory adaptation enzymes.

Results

Two CheR-Mediated Effects on Receptor Sensitivity. We followed control of CheA kinase activity in signaling complexes of the serine chemoreceptor Tsr with a FRET-based in vivo assay of interactions between the response regulator CheY, which obtains phosphoryl groups from CheA, and its phosphatase CheZ (26). We compared Tsr detection sensitivity in an isogenic pair of strains, both of which lacked the CheB sensory adaptation enzyme. One strain (UU2567) also lacked the CheR adaptation enzyme (i.e., R^-B^-); the other strain (UU2697) expressed functional CheR at its native cellular level (i.e., R^+B^-). The serine dose–response data were fitted to a multisite Hill equation to obtain values for the response $K_{1/2}$ (the serine concentration that inhibits 50% of CheA activity), a measure of receptor sensitivity, and the (dimensionless) Hill coefficient, a measure of response cooperativity. The FRET assay also provides a value for the overall receptor-dependent kinase activity in the cells.

The conventional effect of the CheR methyltransferase on receptor sensitivity is illustrated in Fig. 2, *Upper*. Wild-type Tsr subunits are translated with a [QEQEE] pattern of glutaminyl (Q) and glutamyl (E) residues at their five adaptational modification sites (Fig. 1). In Tsr dimers E sites bias receptor output toward a kinase-OFF state, whereas Q residues mimic methylated E sites (Em) and shift output toward a kinase-ON state (1, 9). In UU2567 (R^-B^-), wild-type Tsr subunits encoded by plasmid pPA114 or plasmid pRR53 retain their [QEQEE] residue pattern and produce a serine response with a $K_{1/2}$ of ∼17 μM. In UU2697 (R^+B^-), CheR converts E sites to glutamyl-methylesters (Em), increasing the average methylation state of the Tsr molecules and raising their serine response $K_{1/2}$ to ∼50 μM (Fig. 2, *Upper*). Thus, CheR-mediated methylation shifts wild-type Tsr molecules toward the kinase-ON state and reduces the detection sensitivity of their response to serine.

Tsr molecules with a mutationally imposed [QQQQE] residue pattern at the adaptation sites have more on-shifted character than wild-type Tsr and exhibited a serine response $K_{1/2}$ of ∼160 μM in the UU2567 (R^-B^-) host (Fig. 2, *Lower*). However, in the UU2697 (R^+B^-) host, the Tsr [QQQQE] response $K_{1/2}$ was only ∼40 μM. Although Tsr [QQQQE] has one potential methylation site (E502) (8), it is less reactive than the other four sites and undergoes little modification in UU2697 (R^+B^-) (9). It appears, therefore, that CheR can enhance the response sensitivity of a receptor molecule that has little potential for CheR-mediated modification. We refer to this paradoxical behavior as CheR-enhanced sensitivity. Note that wild-type Tsr [QEQEE] also seems to be subject to the CheR enhancement effect because its serine response $K_{1/2}$ in the $CheR^+$ host is comparable to that of Tsr [QQQQE], and evidently reflects a compromise between the ON-shifting effect of a higher methylation state and the OFF-shifting effect of CheR enhancement (Fig. 2).

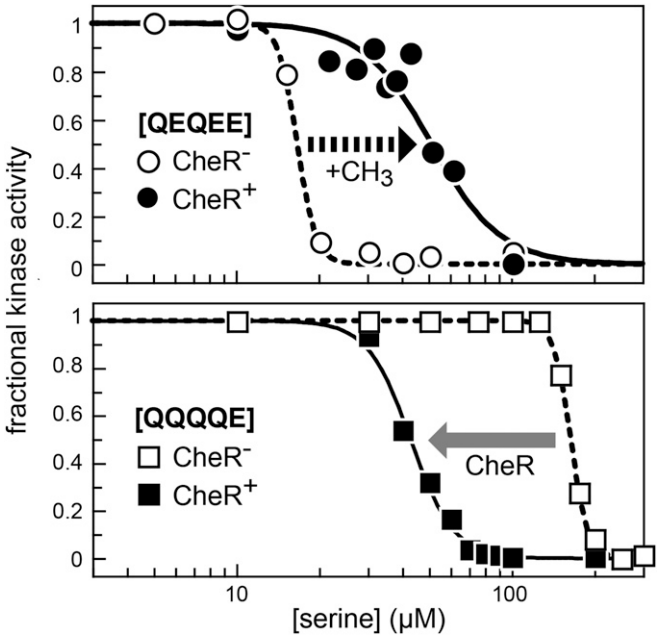

Fig. 2. An example of CheR enhanced response sensitivity. Panels show Hill fits of serine dose–response data obtained from in vivo FRET kinase assays in host strains UU2567 (R^-B^-; white symbols), which lacks both the CheR and CheB adaptation enzymes, and strain UU2697 (R^+B^-; black symbols), which lacks CheB but contains functional CheR. See *SI Appendix*, Table S2 for parameter values. (*Upper*) Behavior of Tsr ([QEQEE]) expressed from plasmid pRR53. (*Lower*) Behavior of Tsr [QQQQE] expressed from a derivative of plasmid pRR53.

To explore the generality of the CheR enhancement effect, we compared the serine response sensitivities in UU2567 (R^-B^-) and UU2697 (R^+B^-) of Tsr variants that had different potentials for methylation by CheR (Fig. 3). We observed the enhancement effect in receptors with as many as two to three available modification sites, some of which could readily undergo CheR-mediated methylation. For example, Tsr-L263F, with a residue change at the C terminus of the HAMP AS2 helix (Fig. 1), has a [QEQEE] adaptation site pattern and is a good substrate for CheR-mediated methylation (*SI Appendix*, Fig. S1), but nevertheless its response $K_{1/2}$ was about threefold lower in the UU2697 (R^+B^-) host (~200 μM) than in the UU2567 (R^-B^-) host (~700 μM) (Fig. 3 and *SI Appendix*, Table S2). Similarly, Tsr-Q311M and Tsr-Q311P, with amino acid replacements at modification site 3 in the MH1 helix (Fig. 1), undergo CheR-mediated methylation (27), but show more than a 10-fold increase in response sensitivity in the host containing CheR (Fig. 3 and *SI Appendix*, Table S2). Receptors with as few as zero to one available modification sites also exhibited CheR-enhanced response sensitivity (Fig. 3). For example, Tsr [NDNDX] receptors with various amino acid replacements at modification site 5 have no known CheR-modifiable sites: D mimics the signaling effects of E (and N mimics the signaling effects of Q), but D residues do not undergo CheR-mediated methylation (9, 28). However, these receptors exhibited enhanced response sensitivity in the CheR-containing UU2697 (R^+B^-) host (Fig. 3 and *SI Appendix*, Table S2). Evidently, CheR-mediated methylation at any of the Tsr glutamyl residue modification sites is not essential for the response enhancement effect.

The $K_{1/2}$ values for the nine receptor variants that responded to serine in both hosts (Fig. 3 and *SI Appendix*, Table S2) averaged about fourfold lower in the CheR-containing host (mean ratio = 0.23; SD = 0.11). The enhanced responses were less cooperative (mean ratio of Hill coefficients = 0.56 ± 0.34), but the prestimulus kinase activities in the two hosts were generally comparable (mean ratio of kinase activities = 1 ± 0.4).

Mechanistic Interpretation of CheR Response Enhancement. In terms of a two-state receptor model (29), attractant stimuli and sensory adaptation shift receptor signaling complexes between a kinase-activating (ON) state with low ligand affinity and a kinase-deactivating (OFF) state with high ligand affinity. Receptor molecules in the ON conformation are good substrates for CheB; receptor molecules in the OFF state are good substrates for CheR. Conceivably, the CheR enhancement effect might occur through CheR-receptor binding interactions that increase the equilibrium proportion of receptor signaling complexes in the OFF state. (See *SI Appendix* for an analysis of the affinity difference this equilibrium binding mechanism would require.)

This CheR equilibrium binding model predicts that the enhancement effect should scale with CheR levels in the cell. Moreover, because response enhancement occurs at the low native CheR:receptor stoichiometry, the receptors might need to be organized into assistance neighborhoods that allow the same CheR molecule to visit other nearby receptors (30, 31). Enhancement might also depend on receptor molecules having the C-terminal pentapeptide (NWETF) that reversibly tethers CheR to the receptor neighborhood and thereby promotes its interaction with the substrate methylation site helices (32, 33). Finally, we expected that the enhancement effect would not require CheR catalytic activity or any CheR-dependent methylation of the target receptor molecules. We tested these predictions in the following series of experiments.

The Tsr Response Enhancement Effect Scales with Intracellular CheR Level. The native expression level of CheR is only about 140 molecules per cell and the stoichiometry of CheR to receptor dimers is ~1:50 (34, 35). We used a salicylate-inducible *cheR* expression plasmid (pPA810) to vary cellular CheR above

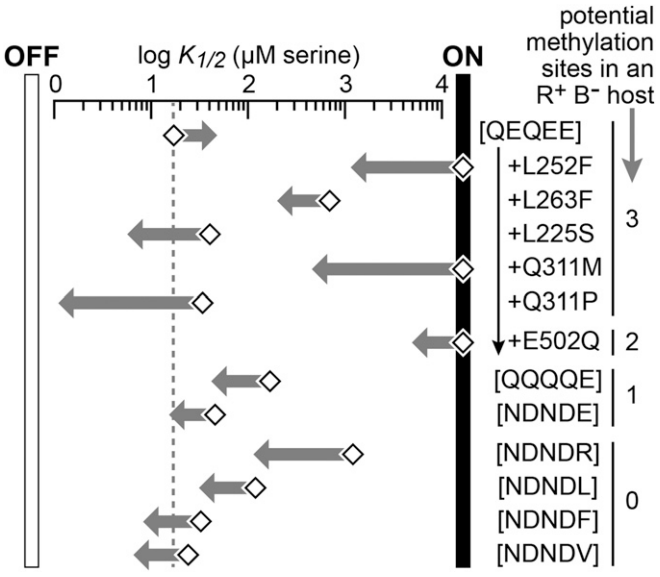

Fig. 3. Examples of Tsr proteins that show CheR-enhanced response sensitivity. Serine dose–response sensitivities of the receptors were determined by in vivo FRET kinase assays in strains UU2567 (R^-B^-; white diamonds) and UU2697 (R^+B^-; dark gray arrowheads). Mutant receptors were expressed from derivatives of plasmids pPA114 (L252F, L263F, L225S, and E502Q) or pRR53 (Q311M, Q311P, [QEQEQ], [QQQQE], [NDNEE], [NDNDR], [NDNDL], [NDNDF], and [NDNDV]). The broken vertical line indicates the response sensitivity of wild-type Tsr [QEQEE] expressed from either plasmid in strain UU2567 (R^-B^-). See *SI Appendix*, Table S2 for parameter values.

the native level. Without induction, pPA810 complemented the chemotaxis defect of a *cheR* deletion mutant and expressed CheR at ~1.5× the native level (*SI Appendix*, Fig. S2). CheR expression from pPA810 rose to ~300× the native level at 0.8 μM salicylate induction (Fig. 4, *Inset*). To assess the influence of CheR expression level on the enhancement effect, we measured the response sensitivity of Tsr [QQQQE] in two Δ(*cheRB*) host strains carrying plasmid pPA810: (*i*) UU2902 expressed Tsr [QQQQE] from a compatible pRR53-derived plasmid and the FRET reporter proteins from inducible chromosomal genes; (*ii*) UU2915 expressed the FRET reporters from a compatible plasmid (pVS88) and Tsr [QQQQE] from the chromosomal *tsr* locus. These strain/plasmid combinations produced comparable results (Fig. 4): The serine response $K_{1/2}$ was ~10-fold lower in cells with uninduced pPA810 than in cells with no CheR (pKG116 vector control) (Fig. 4 and *SI Appendix*, Table S3). With induction up to 0.8 μM salicylate, the $K_{1/2}$ declined approximately fourfold further. Thus, the magnitude of the response enhancement effect scales with cellular CheR level but is effectively saturated at only a few-fold above the native CheR: receptor stoichiometry.

CheR-Mediated Modification of Receptor Adaptation Sites Is Not Required for the Effect. The receptor molecules in the CheR titration experiments above carried a known CheR methylation site, residue E502 (8, 9). To explore the possibility that a low level of E502 modification by CheR might influence the response enhancement effect, we also tested Tsr [QQQQA], carrying an alanine replacement at E502. Tsr-E502A (i.e., a [QEQEA] adaptation site pattern) has signaling properties identical to those of wild-type Tsr ([QEQEE]) in hosts with various combinations

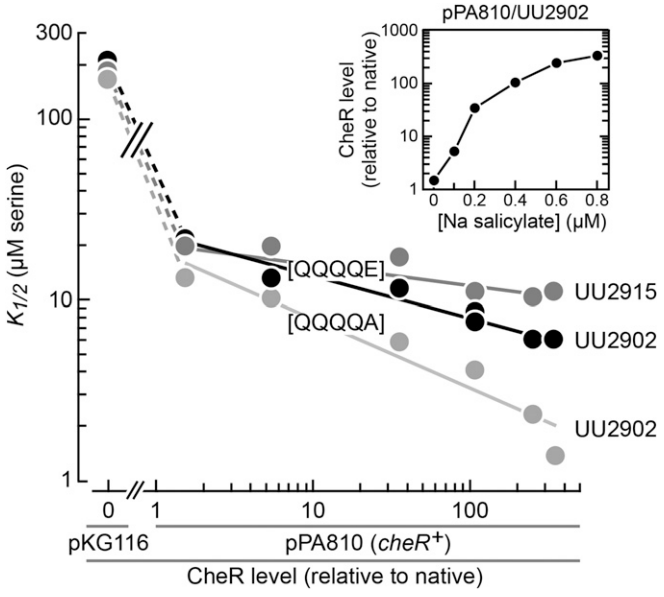

Fig. 4. Dependence of the enhanced response effect on CheR expression level. Serine dose–response sensitivities of wild-type Tsr methylation site variants ([QQQQE] and [QQQQA]) were determined by in vivo FRET kinase assays in CheR⁻ CheB⁻ strains UU2902 [Tsr encoded by plasmid pRR53 derivatives (black or light-gray symbols); FRET reporters expressed from chromosomal loci (YFP-CheY induced with 100 μM xylose; CFP-CheZ induced with 100 μM rhamnose)] and UU2915 [Tsr encoded in chromosome (dark-gray symbols); FRET reporters expressed from pVS88 (induced with 100 μM IPTG)]. Both strains carried a control plasmid (pKG116) or pPA810 to furnish wild-type CheR at various expression levels produced by different concentrations of sodium salicylate inducer (see *Inset* and *SI Appendix*, Table S3). The solid lines are fits to the power function: $K_{1/2} = c \bullet [\text{CheR}]^p$. See *SI Appendix*, Table S3 for parameter values.

of adaptation enzymes (*SI Appendix*, Fig. S3), but cannot undergo CheR-mediated methylation at residue 502 (27). Tsr [QQQQA] showed response sensitivities similar to those of Tsr [QQQQE] over the tested range of CheR expression levels (Fig. 4 and *SI Appendix*, Table S3).

Perhaps CheR has a previously unrecognized, enzymatic activity that can modify Tsr [QQQQA] receptors and shift their output toward the OFF state. We explored this possibility by comparing the electrophoretic mobilities of Tsr [QQQQA] subunits synthesized in cells lacking and containing CheR. Covalent modifications at MCP adaptation sites influence the mobility of receptor subunits in denaturing polyacrylamide gels (23, 36). We observed no mobility shifts in Tsr [QQQQA] molecules from cells with high levels of CheR (*SI Appendix*, Fig. S4). This result rules out the possibility of CheR-mediated deamidation at adaptation sites 1–4 as well as any other covalent modification that detectably shifts receptor subunit mobility. It cannot exclude the possibility that CheR catalyzes a covalent modification of receptor molecules that has no effect on their electrophoretic mobility. Because methylation at E502 evidently plays no substantive role in CheR response enhancement, we used Tsr [QQQQE] to follow the effect in most subsequent experiments.

CheR-Tsr Binding Is Important for the Response Enhancement Effect. The high-abundance receptors in *E. coli* (Tar and Tsr) have a conserved pentapeptide (NWETF) at their C-termini to which CheR binds with ~2 μM affinity (33) (Fig. 5). CheR probably binds to its substrate sites in the receptor methylation helices with lower affinity, because receptor molecules lacking the pentapeptide tether are inefficiently methylated (32). Pentapeptide binding evidently increases the local concentration of CheR in the receptor cluster, enabling one CheR molecule to service groups of neighboring receptors (30, 31). In addition, a structural comparison of apo and pentapeptide-bound forms of CheR suggested that CheR might undergo a conformational change, possibly of functional importance, upon binding the pentapeptide (37).

To assess the contribution to the CheR enhancement effect of the C-terminal pentapeptide on receptor molecules, we compared the response sensitivities of Tsr variants with and without the NWETF pentapeptide. Tsr [QEQEE] ΔNWETF showed comparable response sensitivities in the UU2567 (R^-B^-) and UU2697 (R^+B^-) strains, confirming that the lack of the tether impairs CheR-promoted methylation of wild-type Tsr molecules (*SI Appendix*, Fig. S5 and Table S4). In Tsr [NDNDX] derivatives that undergo CheR-enhanced response sensitivity (Fig. 3) deletion of the NWETF pentapeptide eliminated the enhancement effect (*SI Appendix*, Fig. S5 and Table S4), indicating that response enhancement depends on an interaction between CheR and the NWETF pentapeptide on the receptor molecule. That interaction might directly produce the enhancement effect or it might augment a low-affinity interaction between CheR and the methylation helices of the receptor that is more directly responsible for the effect. To distinguish these possibilities, we measured the response sensitivity of Tsr [QQQQE] ΔNWETF at different CheR expression levels (Fig. 6 and *SI Appendix*, Table S5). The response sensitivity was similar in CheR-deficient cells ($K_{1/2}$ ~ 240 μM) and in cells with a native level of CheR ($K_{1/2}$ ~ 260 μM). However, high-level CheR expression partly compensated for the lack of a tether and enhanced response sensitivity ($K_{1/2}$ ~ 50 μM), demonstrating that the NWETF pentapeptide is not essential to the effect. The tether most likely contributes to the response enhancement effect by promoting binding interactions between CheR and the substrate helices of receptor molecules.

The binding interaction between CheR and its substrate sites in receptor molecules depends on charge interactions between basic residues along one helical face in CheR and acidic residues at or near the receptor methylation sites (38, 39) (Fig. 5). A

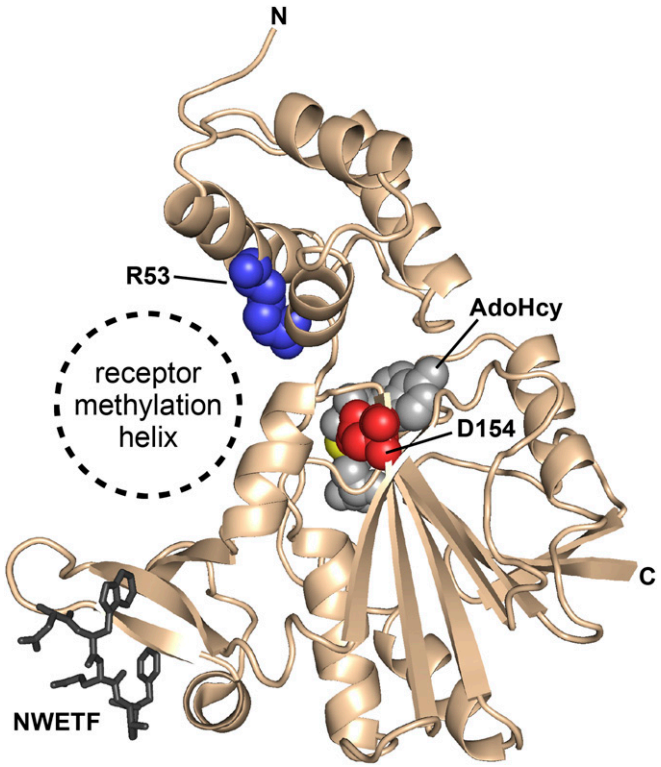

Fig. 5. Structural features of the CheR molecule. Atomic coordinates for the CheR protein of *Salmonella typhimurium* [PDB ID code 1BC5 (42)] were displayed with PyMol software. A few of the native residues at the N terminus (N) and C terminus (C) are not resolved in the crystal structure. Residue R53 (blue, space-filled) plays a role in recognition and binding of the substrate receptor helix (39); residue D154 (red, space-filled) hydrogen bonds with the hydroxyl groups of the ribose ring of the AdoMet methyl donor. The end product of the methyltransferase reaction (AdoHcy: gray, space-filled), is shown bound at the reaction site. Its sulfur atom (yellow, mostly hidden) indicates the location of the methyl group from AdoMet that is transferred to a receptor methylation site in the substrate helix (putative location indicated by the dashed circular outline). The receptor's C-terminal pentapeptide (NWETF) binds to a small auxiliary domain on CheR to tether the methyltransferase in the vicinity of its target substrates (33, 37). The tether function can be supplied by a different, nearby receptor molecule (30, 31).

glutamic acid replacement at CheR residue R53, a putative receptor-binding determinant (39) (Fig. 5), eliminated the CheR enhancement effect (Fig. 6 and *SI Appendix*, Table S5), consistent with the idea that response enhancement occurs through a binding interaction between CheR and the substrate helices of receptor molecules.

CheR Enzymatic Activity Is Not Needed for the Response Enhancement Effect. The methyl donor for the receptor methylation reaction, the only known enzymatic activity of CheR, is S-adenosyl methionine (AdoMet) (40, 41). If a CheR methylation reaction, for example at a heretofore undiscovered receptor site, were important for the response enhancement effect, we reasoned that the effect should be absent in cells starved of methionine, the precursor for AdoMet synthesis (41). That was not the case: The CheR effect persisted in methionine-starved cells (Fig. 6 and *SI Appendix*, Table S6), and control experiments confirmed that the starvation procedure had eliminated CheR-dependent receptor methylation (*SI Appendix*, Fig. S6). We conclude that the response enhancement effect does not require an AdoMet-dependent CheR enzymatic activity.

Residue D154 is a critical determinant for AdoMet binding by CheR (42) (Fig. 5). To ask whether AdoMet binding is required for the CheR enhancement effect, we constructed and characterized alanine and leucine replacement mutants at CheR-D154. Both mutant proteins were stably expressed, but failed to methylate Tsr [EEEEE] molecules (*SI Appendix*, Fig. S7). In dose–response tests with Tsr [QQQQE], neither CheR-D154A nor CheR-D154L produced much change in response sensitivity, even at the highest expression level tested (Fig. 6 and *SI Appendix*, Table S6). Given that a CheR receptor-binding interaction is the basis for response enhancement, this result implies that amino acid replacements at residue D154 not only abrogate AdoMet binding, but also impair the receptor-binding conformation of CheR. As suggested by CheR structural studies (37, 42), AdoMet binding to wild-type CheR may allosterically promote its receptor-binding conformation. Because depletion of AdoMet levels by methionine starvation did not prevent the CheR enhancement effect, S-adenosyl homocysteine (AdoHcy) might also allosterically activate CheR for receptor binding.

Cooperative Receptor Clustering Is Not Needed for the Response Enhancement Effect. CheR response enhancement occurs at native CheR:receptor stoichiometries (~1:50), suggesting that each CheR molecule can influence multiple receptors, perhaps through successive binding visits to receptors in an assistance neighborhood or through binding to a receptor that is part of an extended, cooperative signaling team. To explore this issue, we asked whether a mutant CheW protein (CheW-X3: R117D/E121R/F122S) defective in assembling cooperative receptor arrays (43) would abrogate CheR-enhanced response sensitivity. We measured serine responses in strain UU2961 (R^-B^-), which expresses Tsr [QQQQE] and CheW-X3 from chromosomal loci and CheR and the FRET reporter proteins from compatible plasmids. Although the CheW-X3 cooperativity defect was evident in the dose–response behaviors, the CheR enhancement effect persisted (Fig. 7). We conclude that CheR can boost receptor sensitivity in the absence of receptor clustering and high response cooperativity.

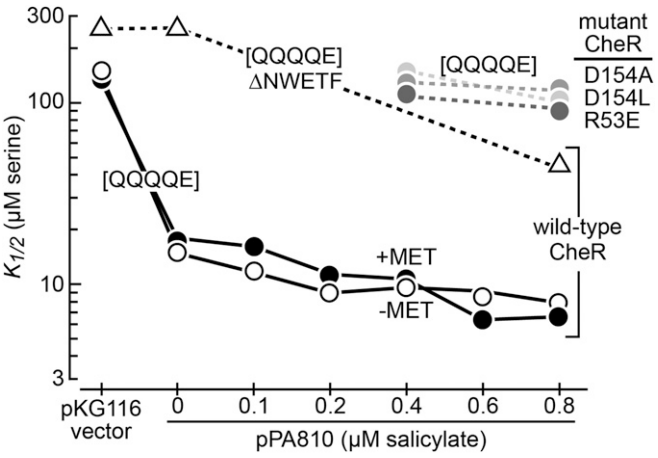

Fig. 6. Roles of receptor binding and methylation in response enhancement by CheR. Serine sensitivities of Tsr [QQQQE] ΔNWETF expressed from a plasmid pRR53 derivative were determined by in vivo FRET kinase assays in strain UU2902 (R^-B^-) carrying plasmid pPA810 or the pKG116 vector (white triangles). Serine sensitivities of Tsr [QQQQE] expressed from a pRR53 derivative were determined in strain UU2902 (R^-B^-) carrying derivatives of plasmid pPA810 to furnish the indicated forms of CheR (D154A: gray symbols; D154L: light-gray symbols; R53E: dark-gray symbols). See *SI Appendix*, Table S5 for parameter values. The effects of methionine starvation were measured in strain UU2967 [Δ(*metF*); R^-B^-], which expresses Tsr [QQQQE] from the chromosomal *tsr* locus, and carried compatible plasmids for the FRET reporter proteins (pVS88) and for CheR (pPA810). One cell sample was starved for methionine (white symbols); a second sample was not (black symbols). See *SI Appendix*, Tables S5 and S6 for parameter values.

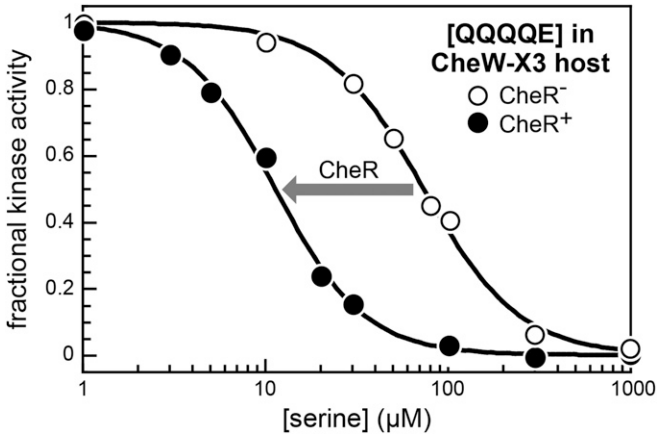

Fig. 7. Response enhancement effect in a receptor array interface 2 mutant host. Serine dose–response sensitivities were determined by in vivo FRET kinase assays of strain UU2961 (Tsr [QQQQE]; CheW-X3; R^-) carrying plasmid pKG116 ($CheR^-$, white symbols) or plasmid pPA810 ($CheR^+$), induced at 0.8 μM sodium salicylate (black symbols). Parameter values: $K_{1/2}$ = 74 μM, Hill = 1.7 ($CheR^-$); $K_{1/2}$ = 11 μM, Hill = 1.8 ($CheR^+$).

The CheR Response Enhancement Effect Increases over Time in Nongrowing Cells. All FRET dose–response experiments described above were done with cells taken from exponential growth conditions and placed in buffer. Given that successively higher intracellular CheR levels produced only modest increases in receptor sensitivity (Fig. 4), the receptor molecules in such cells might be heterogeneous with respect to CheR enhancement, with a subpopulation that is relatively refractory to the effect. To explore this possibility, we treated UU2697 (R^+B^-) cells with chloramphenicol to block new receptor synthesis and examined the subsequent time course of their CheR effect (Fig. 8 and *SI Appendix*, Table S7). In the absence of new receptor synthesis, we found that the response $K_{1/2}$ of Tsr [QQQQE] and Tsr [QQQQA] receptors decreased over time in the $CheR^+$ UU2697 strain (R^+B^-), but remained constant and substantially higher in a $CheR^-$ control strain (UU2567; R^-B^-). The number of receptor molecules in the cells remained essentially constant over the experimental time course (*SI Appendix*, Fig. S8), implying that receptor molecules became more sensitive to the enhancement effect over time or that a transient CheR binding interaction produced a long-lasting change in receptor molecules that rendered them more sensitive to a serine stimulus. We make the case for this latter scenario in the *Discussion*.

Discussion

The CheR Response Enhancement Effect. We have found that both wild-type and mutant serine chemoreceptors exhibit substantially higher detection sensitivity in cells containing the receptor methyltransferase CheR than in cells lacking CheR. This response enhancement effect runs counter to the signaling effects of CheR-mediated covalent modifications, which shift receptor molecules to a kinase-ON state and reduce their sensitivity to attractant ligands. The mechanism of CheR response enhancement is distinct from receptor methylation: It can occur with receptors that have no available modification sites and in methionine-starved cells that have little AdoMet, the methyl donor for the CheR methyltransferase reaction. However, the effect does seem to involve a binding interaction between CheR and the receptor. Tsr molecules lacking the C-terminal CheR-binding pentapeptide failed to show an enhancement effect at native CheR expression levels. The lack of a tether was offset to some extent at increased levels of CheR, indicating that the tether itself is not essential for the enhancement effect. Rather, it probably serves to increase local CheR concentration in receptor signaling complexes, likely promoting a binding interaction to the receptor methylation helices that directly produces the effect. Indeed, a mutant CheR protein defective in interacting with the receptor methylation helices did not produce response enhancement.

Difficulties with an Equilibrium Binding Mechanism for CheR Response Enhancement. In the absence of CheR, equilibrium explanations for the serine-driven ON to OFF kinase activity switch in Tsr signaling complexes require that serine bind more tightly to the OFF state than to the ON state (44–46). A simple extension of this equilibrium approach to encompass the CheR effect would require CheR binding to effectively enhance the serine affinity of the OFF state. The most straightforward way to accomplish this change in effective affinity would be to have CheR itself bind more tightly to the OFF state than to the ON state. At high expression levels, CheR promoted a roughly 40-fold drop in the response $K_{1/2}$ for serine. As illustrated in *SI Appendix*, a simple equilibrium explanation for the enhancement effect without cooperativity would require CheR to bind about 40-fold tighter to the OFF state than to the ON state.

There is both theoretical and experimental support for preferential substrate binding by CheR. Feedback control of the sensory adaptation process through differential recognition of receptor activity states is a critical feature of perfect adaptation models (10–12). Moreover, in vivo and in vitro studies have shown that CheB, the methylesterase, acts on receptors that have a kinase-on state, whereas CheR operates on receptors that have a kinase-OFF state (reviewed in ref. 7). The simplest basis for differential substrate recognition by the sensory adaptation enzymes would be preferential binding to receptors in the preferred signaling state (Fig. 1).

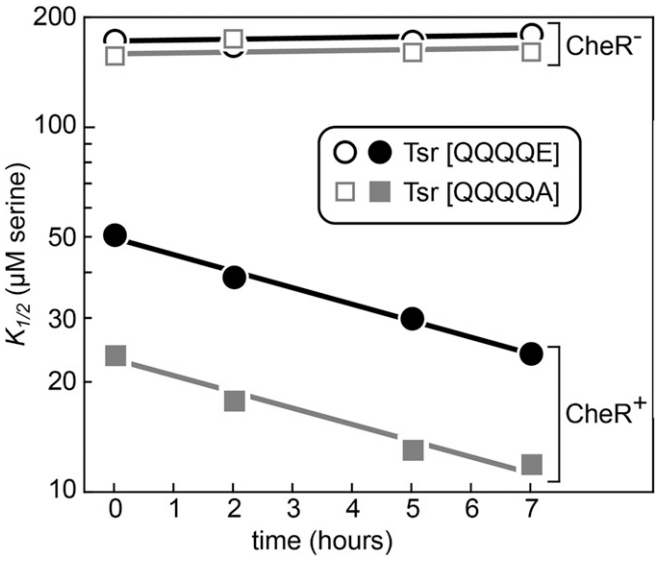

Fig. 8. Time course of the CheR enhancement effect upon cessation of new receptor synthesis. UU2567 ($CheR^-$) and UU2697 ($CheR^+$) cells containing plasmid pRZ30 encoding FRET reporter proteins and pRR53 derivatives encoding Tsr [QQQQE] or Tsr [QQQQA] were grown and prepared for FRET kinase experiments (see *Experimental Procedures*). Cells were then returned to tryptone broth containing no IPTG inducer and 500 μg/mL chloramphenicol to block further protein synthesis and incubated with shaking at 30 °C. At various times thereafter, cells were removed for FRET experiments to measure their response $K_{1/2}$ to serine. Lines are best-fits to a single-exponential function. See *SI Appendix*, Fig. S8 for control data that show the effects of chloramphenicol treatment on intracellular Tsr levels and cell culture densities over the experimental time course. See *SI Appendix*, Table S7 for parameter values.

The principal weakness in an equilibrium binding explanation for the CheR enhancement effect is that the cellular stoichiometry of CheR to receptors is only about 1:50 and yet the enhancement effect is nearly maximal at the native CheR expression level. Thus, in the absence of cooperativity, equilibrium binding interactions between CheR and only a small fraction of the cell's receptors would need to produce the effect. Cooperative interactions within a signaling array could conceivably amplify CheR action, but mutant cells with an array interface 2 lesion (CheW-X3) that disperses signaling complexes and diminishes response cooperativity still showed CheR-enhanced responses (Fig. 7). It follows that the equilibrium effect would need to act on individual signaling units because it does not depend on the amplification effects possible in a large cooperative array.

The fundamental chemoreceptor signaling unit consists of six receptor dimers (organized in two trimers of dimers), one CheA kinase dimer, and two molecules of CheW (47). The asymmetric receptor interfaces in the core complex imply that not all six of the receptor dimers are functionally equivalent. If only one receptor of the core unit were recognized in the OFF signaling state, the stoichiometry of CheR to recognized receptor would be reduced from 1:50 to about 1:8, but this is still not enough to account for a nearly maximal enhancement effect at native CheR:receptor stoichiometry. It seems that the only scenario that could allow an equilibrium binding mechanism for the CheR effect would be if 80–90% of the cell's receptor molecules were not incorporated into signaling complexes and were also incapable of competing with the minority of functional receptors for CheR binding. Current understanding of the chemotaxis machinery makes this scenario implausible (48–52).

A Possible Nonequilibrium Mechanism for CheR Response Enhancement. The low native cellular stoichiometry of CheR to receptor molecules suggests that CheR might act in catalytic fashion to produce the enhancement effect. Although a binding interaction between CheR and the substrate helices of receptor molecules is important to the mechanism, the known catalytic activity of CheR is not. These properties argue against a CheR-catalyzed covalent modification, at any of the known adaptation sites, that acts in opposition to receptor methylation. Rather, the types of receptor alterations that potentiate the effect suggest an alternative mechanism. To date, we have observed CheR enhancement most clearly with mutant receptors that bear structural changes in the methylation site helices or in the adjoining HAMP domain (9, 27). Structural changes in the receptor's hairpin tip region (Fig. 1) that produce a wide range of signaling behaviors did not potentiate the CheR effect (53–55). Perhaps the receptor methylation helices, whose conformation and packing stability are under direct control by the HAMP domain, are central to the CheR effect. We suggest that in the absence of CheR, receptor molecules fold into a kinetically trapped structure that is not the most stable one possible. A CheR binding interaction at the methylation helices promotes the structural change needed to reach a more stable receptor conformation, one that has a higher binding affinity for attractant ligands.

We cannot yet say what the kinetically trapped and CheR-catalyzed receptor structures might be, but the essence of the mechanism is that the conversion is energy driven, using the higher free energy of the trapped form. Receptor conversion could involve a hitherto undiscovered covalent modification by CheR, but it is also possible to imagine ways in which CheR binding alone could assist a receptor conformational change. A plausible mechanism involving a shift in the relative stabilities of intra- and intersubunit packing interactions in the vicinity of the methylation helices is shown in Fig. 9. Even if there is no appreciable reverse reaction, there is continual synthesis of new, unconverted receptor molecules in a CheR-containing cell, so it is also difficult to assess the steady-state number of converted receptor molecules. Considering the lower cooperativity of CheR-enhanced responses, it seems likely that the receptor population is to some extent heterogeneous. This scenario predicts that the CheR effect should continue to enhance response sensitivity in cells that have ceased synthesizing new receptor molecules. Consistent with this prediction, the magnitude of the enhancement effect increased slowly over time in cells treated with chloramphenicol to block further protein synthesis (Fig. 8 and *SI Appendix*, Table S7).

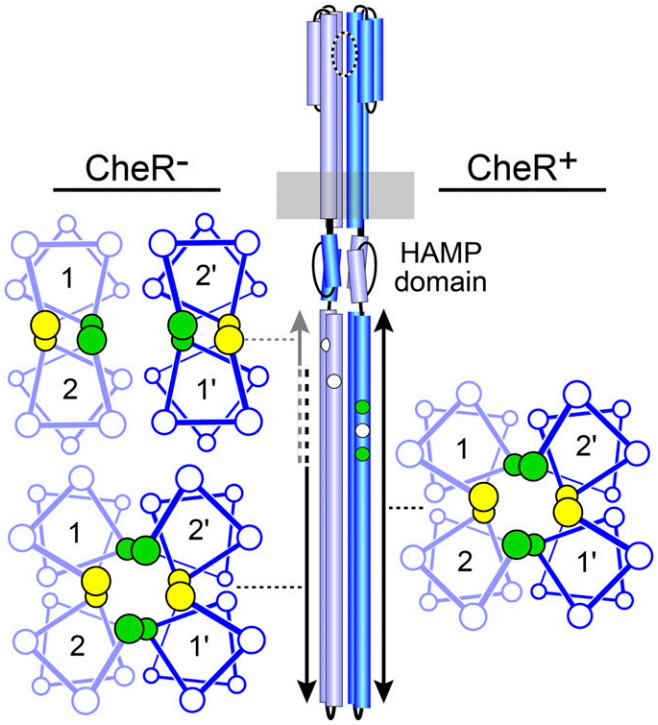

Fig. 9. A possible nonequilibrium mechanism for the CheR enhancement effect. This model proposes that receptor dimers made in cells lacking CheR transition from four-helix coiled-coil packing at the hairpin tip to a stable packing arrangement between helices from the same subunit in the vicinity of the HAMP domain. Packing arrangements are indicated in helical wheel diagrams with shaded circles depicting the *a* (yellow) and *d* (green) heptad packing residues characteristic of coiled-coil helix interactions. Reversible CheR binding interactions with the methylation site helices might destabilize the intrasubunit two-helix structures, fostering a stable four-helix packing arrangement throughout the cytoplasmic signaling domain. The HAMP AS2 helices manipulate receptor output through their direct structural connection to the MH1 helices (4). The packing interactions of MH1 helices in the two-helix intrasubunit arrangement may resist HAMP manipulation to a greater extent than the CheR-converted four-helix form, accounting for the CheR response enhancement effect.

Biological Significance of CheR Response Enhancement. Modern-day chemoreceptors require the opposed signaling properties of the CheR and CheB sensory adaptation enzymes to track spatial chemical gradients with high precision and wide dynamic range (10–12, 56). Conceivably, CheR response enhancement, which opposes the signaling effects of CheR-mediated receptor methylation, could have contributed to gradient-tracking behavior before the evolutionary advent of CheB, by enabling cells to detect and respond to low chemoeffector levels. In contemporary chemotaxis systems, where receptors have multiple methylation sites and undergo both methylation and demethylation reactions, the CheR effect might serve to optimally tune receptor sensitivity to different ambient chemoeffector concentrations.

A catalytic mechanism for the CheR enhancement effect raises a number of interesting experimental questions. Do CheR-conditioned receptor molecules show enhanced sensitivity in the absence of

CheR? What is the structural difference between the two proposed receptor OFF states? Are receptor molecules able to reach the higher affinity conformational state without CheR assistance? These questions should be addressed in additional studies.

Experimental Procedures

Bacterial Strains and Plasmids. Strains used in this study were derivatives of *E. coli* K-12 strain RP437 (57). Their relevant genotypes are listed in *SI Appendix*, Table S1. The plasmids used in this work were: pKG116, a derivative of pACYC184 that confers chloramphenicol resistance and has a sodium salicylate-inducible expression/cloning site (58); pPA810, a derivative of pKG116 that carries *cheR* under salicylate control; pPA114, a derivative of pKG116 that expresses Tsr under salicylate control (59); pVS88, a derivative of pTrc99A that expresses CheY-YFP and CheZ-CFP under isopropyl-β-D-thiogalactopyranoside (IPTG)-inducible control (26); and pRR53, a derivative of pBR322 that expresses Tsr under IPTG control (59).

Site-Directed Mutagenesis. Mutations in various plasmids were generated using Agilent QuikChange PCR Mutagenesis and verified by sequencing the entire coding region of the targeted genes, as previously described (59).

Expression Levels of CheR Proteins. CheR expression from pPA810 was measured in strain UU2902; native CheR expression was measured in strain RP437. Cell samples were prepared as described by Li and Hazelbauer (34) and analyzed by SDS/PAGE and immunoblotting, as described previously (34, 54). Briefly, cells were grown in tryptone broth (containing 12.5 μg/mL chloramphenicol and different concentrations of sodium salicylate inducer for pPA810 experiments) at 30 °C to OD600 = 0.5. Cells (1 mL) were harvested and lysed by adding 200 μL of 50% (wt/wt) ice-cold trichloroacetic acid (TCA), incubating on ice for 15 min, and centrifuging for 15 min at 16,000 × *g* at 4 °C. The TCA pellet was then washed by vortexing with 1 mL ice-cold acetone, centrifuged as before, air dried after discarding the supernatant, and resuspended in 100 μL SDS sample buffer. Native CheR samples were concentrated fivefold more than those from plasmid-expressed CheR samples. Immunoblots were incubated at room temperature overnight, using a 1:500 dilution of CheR antiserum provided by Ann Stock, University of Medicine and Dentistry of New Jersey, Newark, NJ, and Rutgers University, New Brunswick, NJ.

FRET-Based Measurement of in Vivo Kinase Activity. The assay protocol and data analysis followed the procedures previously described in detail (26, 60).

Methionine Starvation Protocol. Strains with a *ΔmetF* mutation (UU2967 or UU2970) were grown and starved for methionine as described previously (41). Briefly, cells were grown to OD600 = 0.5 in tryptone broth at 30 °C, harvested by centrifuging at ~1,100 × *g* for 6 min, washed twice with equal volumes of wash medium (10 mM potassium phosphate buffer at pH 7.0, 0.1 mM EDTA, 10 mM sodium lactate, and 0.1 mM each of threonine, leucine and histidine), and resuspended in an equal volume of wash medium. Cells were then incubated at 30 °C with aeration for 60 min to starve them for methionine before use in FRET assays.

ACKNOWLEDGMENTS. We thank Ann Stock for CheR antiserum and for advice on CheR experiments; and Claudia Studdert, David Blair, Kelly Hughes, Tom Shimizu, and Ady Vaknin for comments on the manuscript. This work was supported by National Institute of General Medical Sciences Grants GM19559 (to J.S.P.) and GM59544 (to F.W.D.). The Protein-DNA Core Facility at the University of Utah receives support from National Cancer Institute Grant CA42014 to the Huntsman Cancer Institute.

1. Hazelbauer GL, Falke JJ, Parkinson JS (2008) Bacterial chemoreceptors: High-performance signaling in networked arrays. *Trends Biochem Sci* 33:9–19.
2. Parkinson JS, Hazelbauer GL, Falke JJ (2015) Signaling and sensory adaptation in *Escherichia coli* chemoreceptors: 2015 update. *Trends Microbiol* 23:257–266.
3. Alexander RP, Zhulin IB (2007) Evolutionary genomics reveals conserved structural determinants of signaling and adaptation in microbial chemoreceptors. *Proc Natl Acad Sci USA* 104:2885–2890.
4. Parkinson JS (2010) Signaling mechanisms of HAMP domains in chemoreceptors and sensor kinases. *Annu Rev Microbiol* 64:101–122.
5. Koshland DE, Jr (1980) Bacterial chemotaxis in relation to neurobiology. *Annu Rev Neurosci* 3:43–75.
6. Adler J (1983) Bacterial chemotaxis and molecular neurobiology. *Cold Spring Harb Symp Quant Biol* 48:803–804.
7. Hazelbauer GL, Lai WC (2010) Bacterial chemoreceptors: Providing enhanced features to two-component signaling. *Curr Opin Microbiol* 13:124–132.
8. Rice MS, Dahlquist FW (1991) Sites of deamidation and methylation in Tsr, a bacterial chemotaxis sensory transducer. *J Biol Chem* 266:9746–9753.
9. Han XS, Parkinson JS (2014) An unorthodox sensory adaptation site in the *Escherichia coli* serine chemoreceptor. *J Bacteriol* 196:641–649.
10. Alon U, Surette MG, Barkai N, Leibler S (1999) Robustness in bacterial chemotaxis. *Nature* 397:168–171.
11. Barkai N, Leibler S (1997) Robustness in simple biochemical networks. *Nature* 387:913–917.
12. Yi TM, Huang Y, Simon MI, Doyle J (2000) Robust perfect adaptation in bacterial chemotaxis through integral feedback control. *Proc Natl Acad Sci USA* 97:4649–4653.
13. Kehry MR, Engström P, Dahlquist FW, Hazelbauer GL (1983) Multiple covalent modifications of Trg, a sensory transducer of *Escherichia coli*. *J Biol Chem* 258:5050–5055.
14. Terwilliger TC, Wang JY, Koshland DE, Jr (1986) Surface structure recognized for covalent modification of the aspartate receptor in chemotaxis. *Proc Natl Acad Sci USA* 83:6707–6710.
15. Nowlin DM, Bollinger J, Hazelbauer GL (1987) Sites of covalent modification in Trg, a sensory transducer of *Escherichia coli*. *J Biol Chem* 262:6039–6045.
16. Starrett DJ, Falke JJ (2005) Adaptation mechanism of the aspartate receptor: Electrostatics of the adaptation subdomain play a key role in modulating kinase activity. *Biochemistry* 44:1550–1560.
17. Winston SE, Mehan R, Falke JJ (2005) Evidence that the adaptation region of the aspartate receptor is a dynamic four-helix bundle: Cysteine and disulfide scanning studies. *Biochemistry* 44:12655–12666.
18. Zhou Q, Ames P, Parkinson JS (2009) Mutational analyses of HAMP helices suggest a dynamic bundle model of input-output signalling in chemoreceptors. *Mol Microbiol* 73:801–814.
19. Zhou Q, Ames P, Parkinson JS (2011) Biphasic control logic of HAMP domain signalling in the *Escherichia coli* serine chemoreceptor. *Mol Microbiol* 80:596–611.
20. Goy MF, Springer MS, Adler J (1977) Sensory transduction in *Escherichia coli*: Role of a protein methylation reaction in sensory adaptation. *Proc Natl Acad Sci USA* 74:4964–4968.
21. Stock JB, Koshland DE, Jr (1978) A protein methylesterase involved in bacterial sensing. *Proc Natl Acad Sci USA* 75:3659–3663.
22. Rollins C, Dahlquist FW (1981) The methyl-accepting chemotaxis proteins of *E. coli*: A repellent-stimulated, covalent modification, distinct from methylation. *Cell* 25:333–340.
23. Sherris D, Parkinson JS (1981) Posttranslational processing of methyl-accepting chemotaxis proteins in *Escherichia coli*. *Proc Natl Acad Sci USA* 78:6051–6055.
24. Parkinson JS, Revello PT (1978) Sensory adaptation mutants of *E. coli*. *Cell* 15:1221–1230.
25. Yonekawa H, Hayashi H, Parkinson JS (1983) Requirement of the *cheB* function for sensory adaptation in *Escherichia coli*. *J Bacteriol* 156:1228–1235.
26. Sourjik V, Vaknin A, Shimizu TS, Berg HC (2007) In vivo measurement by FRET of pathway activity in bacterial chemotaxis. *Methods Enzymol* 423:365–391.
27. Han XS (2015) Control of serine receptor signaling by the sensory adaptation system in *Escherichia coli*. PhD dissertation (University of Utah, Salt Lake City).
28. Shapiro MJ, Chakrabarti I, Koshland DE, Jr (1995) Contributions made by individual methylation sites of the *Escherichia coli* aspartate receptor to chemotactic behavior. *Proc Natl Acad Sci USA* 92:1053–1056.
29. Asakura S, Honda H (1984) Two-state model for bacterial chemoreceptor proteins. The role of multiple methylation. *J Mol Biol* 176:349–367.
30. Le Moual H, Quang T, Koshland DE, Jr (1997) Methylation of the *Escherichia coli* chemotaxis receptors: Intra- and interdimer mechanisms. *Biochemistry* 36:13441–13448.
31. Li J, Li G, Weis RM (1997) The serine chemoreceptor from *Escherichia coli* is methylated through an inter-dimer process. *Biochemistry* 36:11851–11857.
32. Feng X, Lilly AA, Hazelbauer GL (1999) Enhanced function conferred on low-abundance chemoreceptor Trg by a methyltransferase-docking site. *J Bacteriol* 181:3164–3171.
33. Wu J, Li J, Li G, Long DG, Weis RM (1996) The receptor binding site for the methyltransferase of bacterial chemotaxis is distinct from the sites of methylation. *Biochemistry* 35:4984–4993.
34. Li M, Hazelbauer GL (2004) Cellular stoichiometry of the components of the chemotaxis signaling complex. *J Bacteriol* 186:3687–3694.
35. Simms SA, Stock AM, Stock JB (1987) Purification and characterization of the S-adenosylmethionine:glutamyl methyltransferase that modifies membrane chemoreceptor proteins in bacteria. *J Biol Chem* 262:8537–8543.
36. Engström P, Hazelbauer GL (1980) Multiple methylation of methyl-accepting chemotaxis proteins during adaptation of *E. coli* to chemical stimuli. *Cell* 20:165–171.
37. Djordjevic S, Stock AM (1998) Chemotaxis receptor recognition by protein methyltransferase CheR. *Nat Struct Biol* 5:446–450.
38. Perez E, West AH, Stock AM, Djordjevic S (2004) Discrimination between different methylation states of chemotaxis receptor Tar by receptor methyltransferase CheR. *Biochemistry* 43:953–961.
39. Shiomi D, Okumura H, Homma M, Kawagishi I (2000) The aspartate chemoreceptor Tar is effectively methylated by binding to the methyltransferase mainly through hydrophobic interaction. *Mol Microbiol* 36:132–140.
40. Kort EN, Goy MF, Larsen SH, Adler J (1975) Methylation of a membrane protein involved in bacterial chemotaxis. *Proc Natl Acad Sci USA* 72:3939–3943.
41. Springer MS, Goy MF, Adler J (1977) Sensory transduction in *Escherichia coli*: A requirement for methionine in sensory adaptation. *Proc Natl Acad Sci USA* 74:183–187.

42. Djordjevic S, Stock AM (1997) Crystal structure of the chemotaxis receptor methyltransferase CheR suggests a conserved structural motif for binding S-adenosylmethionine. *Structure* 5:545–558.
43. Piñas GE, Frank V, Vaknin A, Parkinson JS (2016) The source of high signal cooperativity in bacterial chemosensory arrays. *Proc Natl Acad Sci USA* 113:3335–3340.
44. Bray D, Levin MD, Morton-Firth CJ (1998) Receptor clustering as a cellular mechanism to control sensitivity. *Nature* 393:85–88.
45. Levit MN, Stock JB (2002) Receptor methylation controls the magnitude of stimulus-response coupling in bacterial chemotaxis. *J Biol Chem* 277:36760–36765.
46. Sourjik V, Berg HC (2004) Functional interactions between receptors in bacterial chemotaxis. *Nature* 428:437–441.
47. Li M, Hazelbauer GL (2011) Core unit of chemotaxis signaling complexes. *Proc Natl Acad Sci USA* 108:9390–9395.
48. Briegel A, et al. (2012) Bacterial chemoreceptor arrays are hexagonally packed trimers of receptor dimers networked by rings of kinase and coupling proteins. *Proc Natl Acad Sci USA* 109:3766–3771.
49. Kentner D, Sourjik V (2006) Spatial organization of the bacterial chemotaxis system. *Curr Opin Microbiol* 9:619–624.
50. Liu J, et al. (2012) Molecular architecture of chemoreceptor arrays revealed by cryoelectron tomography of *Escherichia coli* minicells. *Proc Natl Acad Sci USA* 109: E1481–E1488.
51. Maddock JR, Shapiro L (1993) Polar location of the chemoreceptor complex in the *Escherichia coli* cell. *Science* 259:1717–1723.
52. Studdert CA, Parkinson JS (2005) Insights into the organization and dynamics of bacterial chemoreceptor clusters through in vivo crosslinking studies. *Proc Natl Acad Sci USA* 102:15623–15628.
53. Gosink KK, Zhao Y, Parkinson JS (2011) Mutational analysis of N381, a key trimer contact residue in Tsr, the *Escherichia coli* serine chemoreceptor. *J Bacteriol* 193: 6452–6460.
54. Mowery P, Ostler JB, Parkinson JS (2008) Different signaling roles of two conserved residues in the cytoplasmic hairpin tip of Tsr, the *Escherichia coli* serine chemoreceptor. *J Bacteriol* 190:8065–8074.
55. Lai RZ, Gosink KK, Parkinson JS (2017) Signaling consequences of structural lesions that alter the stability of chemoreceptor trimers of dimers. *J Mol Biol* 429:823–835.
56. Meir Y, Jakovljevic V, Oleksiuk O, Sourjik V, Wingreen NS (2010) Precision and kinetics of adaptation in bacterial chemotaxis. *Biophys J* 99:2766–2774.
57. Parkinson JS, Houts SE (1982) Isolation and behavior of *Escherichia coli* deletion mutants lacking chemotaxis functions. *J Bacteriol* 151:106–113.
58. Burón-Barral MC, Gosink KK, Parkinson JS (2006) Loss- and gain-of-function mutations in the F1-HAMP region of the *Escherichia coli* aerotaxis transducer Aer. *J Bacteriol* 188:3477–3486.
59. Ames P, Studdert CA, Reiser RH, Parkinson JS (2002) Collaborative signaling by mixed chemoreceptor teams in *Escherichia coli*. *Proc Natl Acad Sci USA* 99:7060–7065.
60. Lai RZ, Parkinson JS (2014) Functional suppression of HAMP domain signaling defects in the *E. coli* serine chemoreceptor. *J Mol Biol* 426:3642–3655.

SI Appendix

A Two State Equilibrium Model for Receptor Conformational Switching in the Presence of CheR

We assume that chemotaxis receptor signaling complexes can exist in an equilibrium between two states, the kinase-on (ON) or kinase-off (OFF) state. In addition we imagine that the receptor ligand (L) can reversibly bind to the ON or OFF state to form the ON•L and OFF•L states. Similarly, CheR (R) can bind to the ON, ON•L, OFF and OFF•L states of the receptor in an equilibrium fashion to form ON•R, ON•R•L, OFF•R and OFF•R•L states. It is convenient to represent the eight species (shown in blue) potentially present at the vertices of a cube (Fig. 1).

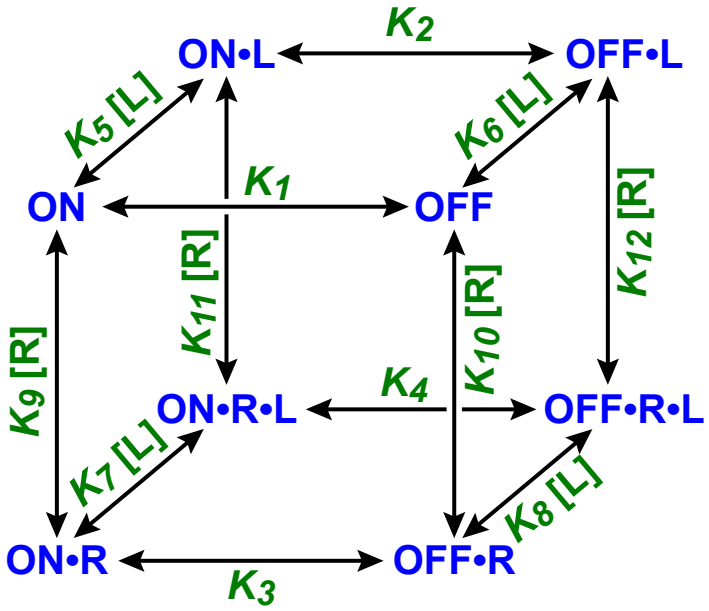

Figure – The eight states of the receptor (blue) in the presence of an attractant ligand (L) and CheR (R) that interconvert by twelve paths defined by pseudo first-order equilibrium constants (green).

Seven independent equilibrium constants are sufficient to define the equilibria among these eight species. The two-headed arrows shown as the edges of the cube define a total of twelve pathways that interconvert the eight states. Each edge is labeled with an equilibrium constant (for isomerizations) or as the product of an association constant and ligand concentration (for binding events). Thus K_5[L] defines the association equilibrium

$$\mathrm{ON} + \mathrm{L} \underset{}{\overset{K_5}{\rightleftharpoons}} \mathrm{ON{\bullet}L} \quad \text{where} \quad K_5 = \frac{[\mathrm{ON{\bullet}L}]}{[\mathrm{ON}][\mathrm{L}]} \quad \text{and} \quad K_5[\mathrm{L}] = \frac{[\mathrm{ON{\bullet}L}]}{[\mathrm{ON}]} \qquad [1]$$

We define the six additional independent equilibrium constants as

$$\mathrm{ON} \underset{}{\overset{K_1}{\rightleftharpoons}} \mathrm{OFF} \qquad K_1 = \frac{[\mathrm{OFF}]}{[\mathrm{ON}]} \qquad [2]$$

$$\mathrm{ON{\bullet}R} \overset{K_3}{\rightleftharpoons} \mathrm{OFF{\bullet}R} \qquad K_3 = \frac{[\mathrm{OFF{\bullet}R}]}{[\mathrm{ON{\bullet}R}]} \qquad [3]$$

$$\mathrm{OFF} + \mathrm{L} \overset{K_6}{\rightleftharpoons} \mathrm{OFF{\bullet}L} \qquad K_6 = \frac{[\mathrm{OFF{\bullet}L}]}{[\mathrm{OFF}][\mathrm{L}]} \qquad [4]$$

$$\mathrm{OFF{\bullet}R} + \mathrm{L} \overset{K_8}{\rightleftharpoons} \mathrm{OFF{\bullet}R{\bullet}L} \qquad K_8 = \frac{[\mathrm{OFF{\bullet}R{\bullet}L}]}{[\mathrm{OFF{\bullet}R}][\mathrm{L}]} \qquad [5]$$

$$\mathrm{OFF{\bullet}L} + \mathrm{R} \overset{K_{12}}{\rightleftharpoons} \mathrm{OFF{\bullet}R{\bullet}L} \qquad K_{12} = \frac{[\mathrm{OFF{\bullet}R{\bullet}L}]}{[\mathrm{OFF{\bullet}L}][\mathrm{R}]} \qquad [6]$$

$$\mathrm{ON} + \mathrm{R} \overset{K_9}{\rightleftharpoons} \mathrm{ON{\bullet}R} \qquad K_9 = \frac{[\mathrm{ON{\bullet}R}]}{[\mathrm{ON}][\mathrm{R}]} \qquad [7]$$

The remaining equilibria shown in Figure 1 can be represented by equations 1-7. For example,

$$\mathrm{OFF} + \mathrm{R} \overset{K_{10}}{\rightleftharpoons} \mathrm{OFF{\bullet}R} \qquad K_{10} = \frac{[\mathrm{OFF{\bullet}R}]}{[\mathrm{OFF}][\mathrm{R}]} \qquad K_{10} = \frac{K_9 K_3}{K_1} \qquad [8a]$$

and

$$\mathrm{ON{\bullet}L} \overset{K_2}{\rightleftharpoons} \mathrm{OFF{\bullet}L} \qquad K_2 = \frac{[\mathrm{OFF{\bullet}L}]}{[\mathrm{ON{\bullet}L}]} \qquad K_2 = \frac{K_1 K_6}{K_5} \qquad [8b]$$

Using the 8 states, we can define the fraction of the receptors that are in the ON and OFF states:

$$\mathit{fraction}\mathrm{ON} = \frac{[\mathrm{ON}] + [\mathrm{ON{\bullet}L}] + [\mathrm{ON{\bullet}R}] + [\mathrm{ON{\bullet}R{\bullet}L}]}{\sum [\text{all forms}]} \qquad [9]$$

$$\mathit{fraction}\mathrm{OFF} = \frac{[\mathrm{OFF}] + [\mathrm{OFF{\bullet}L}] + [\mathrm{OFF{\bullet}R}] + [\mathrm{OFF{\bullet}R{\bullet}L}]}{\sum [\text{all forms}]} \qquad [10]$$

The ratio (*fraction*ON/*fraction*OFF) becomes, upon substituting the equilibrium expressions for the concentrations of various states (and with $L = [\mathrm{L}]$ and $R = [\mathrm{R}]$),

$$\frac{\mathit{fraction}\mathrm{ON}}{\mathit{fraction}\mathrm{OFF}} = \frac{1 + K_5 L + K_9 R + K_9 K_7 R L}{K_1 \{1 + K_6 L + K_{10} R + K_{10} K_8 R L\}} \qquad [11]$$

We assume that the value of $K_{1/2}$ observed in the array interface 2 mutant, where there are no cooperative interactions between core signaling units, reflects the condition that the fraction of core complexes in ON and OFF states is equal. The fact that these mutants show little ligand-driven cooperativity in their dose response curves implies that, effectively, the signaling state of one receptor dominates the signaling state of the core unit so that

$$\frac{1 + K_5L' + K_9R + K_9K_7RL'}{K_1\{1 + K_6L' + K_{10}R + K_{10}K_8RL'\}} = 1 \qquad [12]$$

where L' equals $K_{1/2}$. In the absence of CheR, this reduces to

$$\frac{1 + K_5L'}{K_1\{1 + K_6L'\}} = 1 \qquad [13]$$

and

$$L' = \frac{1 - K_1}{K_1K_6 - K_5} \qquad [14]$$

because of the pathway independence of the equilibria shown in Figure 1,

$$K_1K_6 = K_2K_5 \text{ and } L' = \frac{1 - K_1}{K_5\{K_2 - 1\}} \qquad [15]$$

Under normal conditions, the ON state is favored in the absence of ligands so $K_1 << 1$ and $K_2 >> 1$ because the OFF state is favored when ligand is bound to the receptor, so

$$L' \approx \frac{1}{K_5K_2} \qquad [16]$$

In the presence of CheR, we assume that there is no interaction between CheR binding and ligand binding, *i.e.,* $K_9 = K_{11}$ and $K_{10} = K_{12}$. Arguments similar to the above for the CheR-free case give a solution for the value of L'', the ligand concentration at $K_{1/2}$ in the presence of CheR:

$$L'' \approx \frac{1}{K_5'K_2} \quad \text{where} \quad K_5' = K_5\frac{\{1 + K_9R\}}{\{1 + K_{10}R\}} \qquad [17]$$

The ratio of the value of $K_{1/2}$ observed in the presence versus absence of CheR becomes

$$\frac{L''}{L'} = \frac{1 + K_{10}R}{1 + K_9R} \qquad [18]$$

In the presence of saturating CheR, this becomes

$$\frac{L''}{L'} = \frac{K_{10}}{K_9} \qquad [19]$$

So, in order for CheR to cause the 40-fold decrease in $K_{1/2}$ that we observed, CheR would have to bind 40 times more strongly to the OFF state than to the ON state (see Figure above).

Supplemental Figures

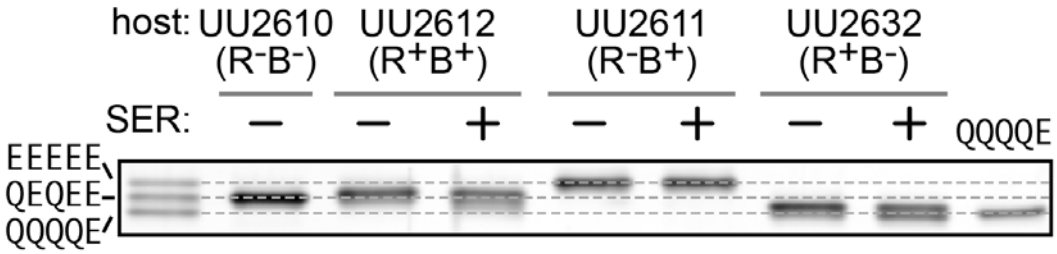

Fig. S1. Adaptational modifications of Tsr-L263F. Lysates of the indicated host strains expressing Tsr-L263F were subjected to electrophoresis in denaturing polyacrylamide gels (SDS-PAGE). Tsr bands were visualized by immuno-blotting with polyclonal anti-Tsr antibodies. The leftmost lane contained a mixture of three reference standards, Tsr [EEEEE], Tsr [QEQEE] and Tsr [QQQQE] prepared in strain UU2610 (R-B-).

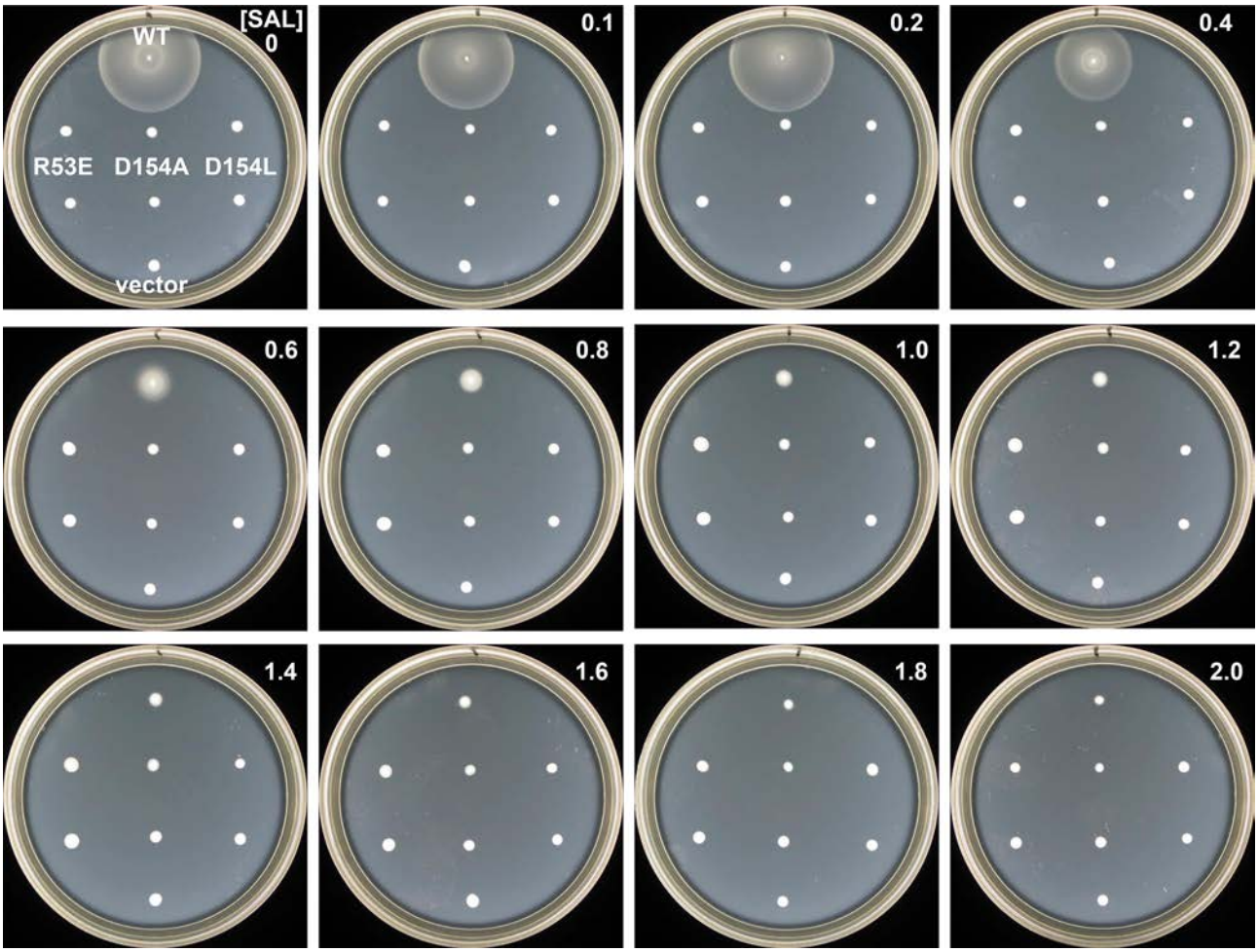

Fig. S2. Complementation of *cheR* function by plasmid pPA810 derivatives. Plasmid pPA810 (wild-type *cheR*) and its mutant derivatives expressing CheR-R53E, CheR-D154A, and CheR-D154L, were tested for ability to support chemotaxis of strain RP4968 [Δ(cheR)] on tryptone semi-solid agar (1% (w/v) tryptone, 0.5% (w/v) NaCl, and 0.25% (w/v) agar) containing 12.5 μg/ml chloramphenicol and the indicated concentrations (in μM) of sodium salicylate inducer. Plates were incubated at 32.5°C for 5.5 hours.

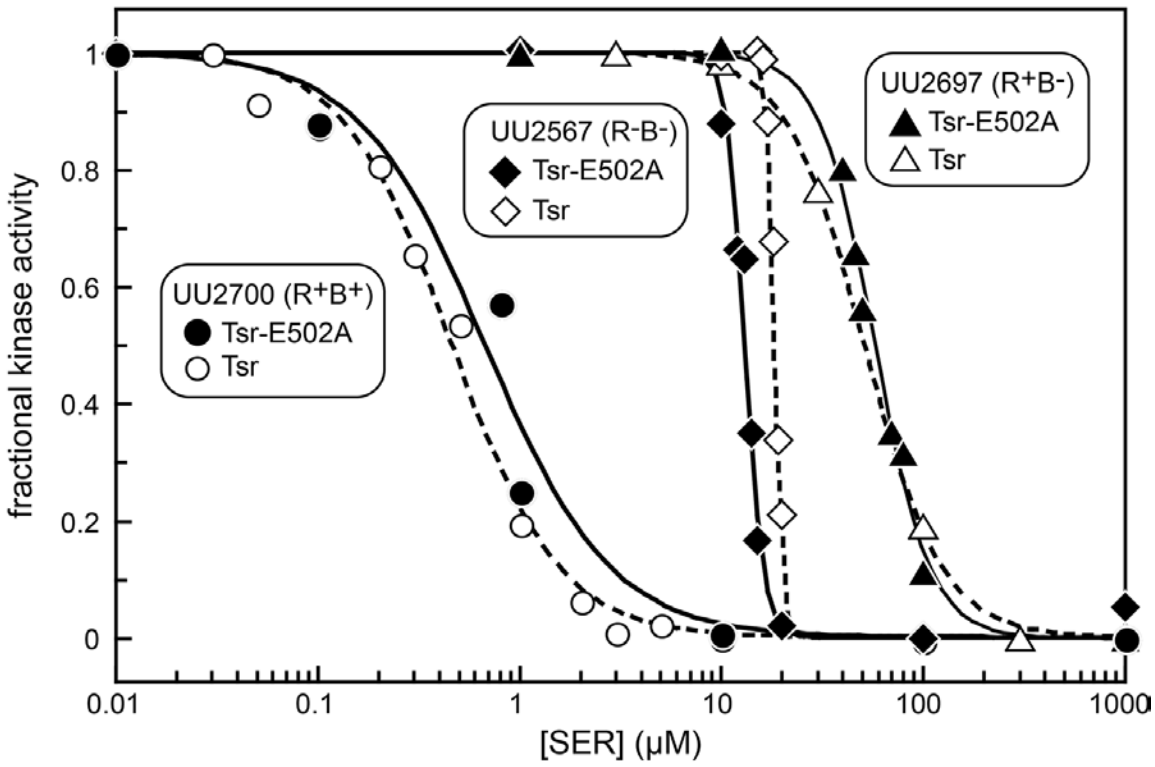

Fig. S3. Comparison of Tsr wild type and Tsr-E502A response parameters in three hosts.

Response data from *in vivo* FRET kinase assays were taken from (27).

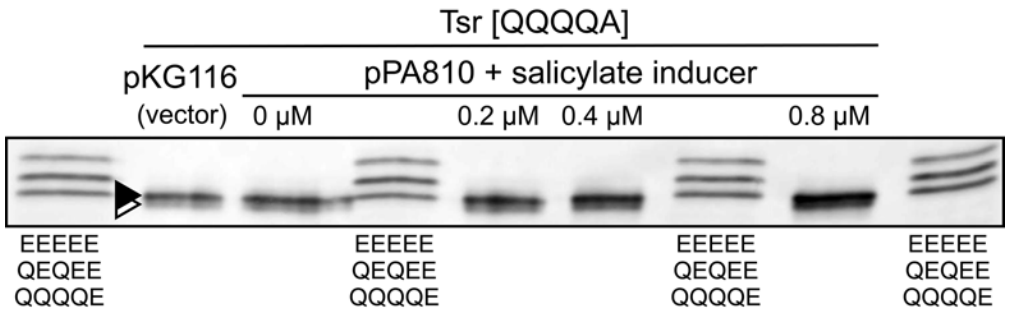

Fig. S4. Comparison of SDS-PAGE mobility of Tsr [QQQQA] subunits from CheR- and CheR+ hosts. Strain UU2567 (R-B-) carried a pRR53 derivative supplying Tsr [QQQQA] at native level and a compatible CheR expression plasmid (pPA810) or its vector control (pKG116). The cells were grown to OD600 = 0.5 at 30°C in tryptone broth containing 50 μg/ml ampicillin, 12.5 μg/ml chloramphenicol, 100 μM IPTG, and salicylate at various concentrations. Protein samples were prepared with minor modifications as previously described (36). Cells were harvested by centrifuging at ~1100 x g for 6 minutes, and washed twice with KEP (10 mM potassium phosphate buffer at pH 7.0, and 0.1 mM EDTA), resuspended in half the original volume of KEP, and aerated by shaking at 30°C for 20 minutes. After the incubation, 450 μl of each cell sample were mixed with 50 μl 100 mM L-serine, and incubated at 30°C for another 20 minutes. Cells were collected by centrifugation at ~9500 x g for 1 minute, and lysed by adding 100 μl SDS sample buffer. Tsr subunits with different modification states were resolved by SDS-PAGE and visualized by immunoblotting as described (54). Tsr [QQQQA] runs as a single band (black triangle) at the same position as the [QQQQE] standard. The faint band (white triangle) in all Tsr lanes is due to a protein that cross-reacts with anti-Tsr serum.

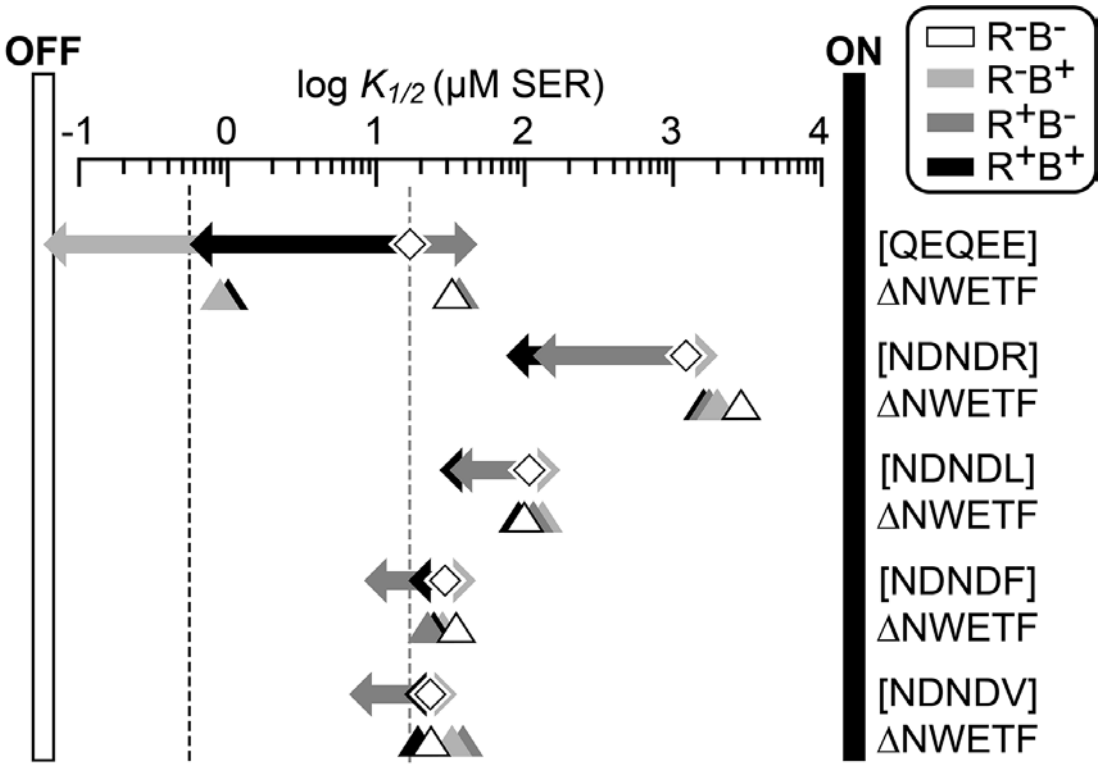

Fig. S5. Response parameters of Tsr wild-type and TsrΔNWETF derivatives in four hosts. Serine dose-responses were measured by FRET kinase assay in four isogenic host strains: UU2567 (R-B-; white diamonds and triangles); UU2699 (R-B+; light gray arrows and triangles); UU2697 (R+B-; dark gray arrows and triangles); UU2700 (R+B+; black arrows and triangles). Broken vertical lines show the response sensitivities for wild-type Tsr in UU2567 (R-B-; gray line) and UU2700 (R+B+; black line). See SI Appendix, Table S4 for parameter values.

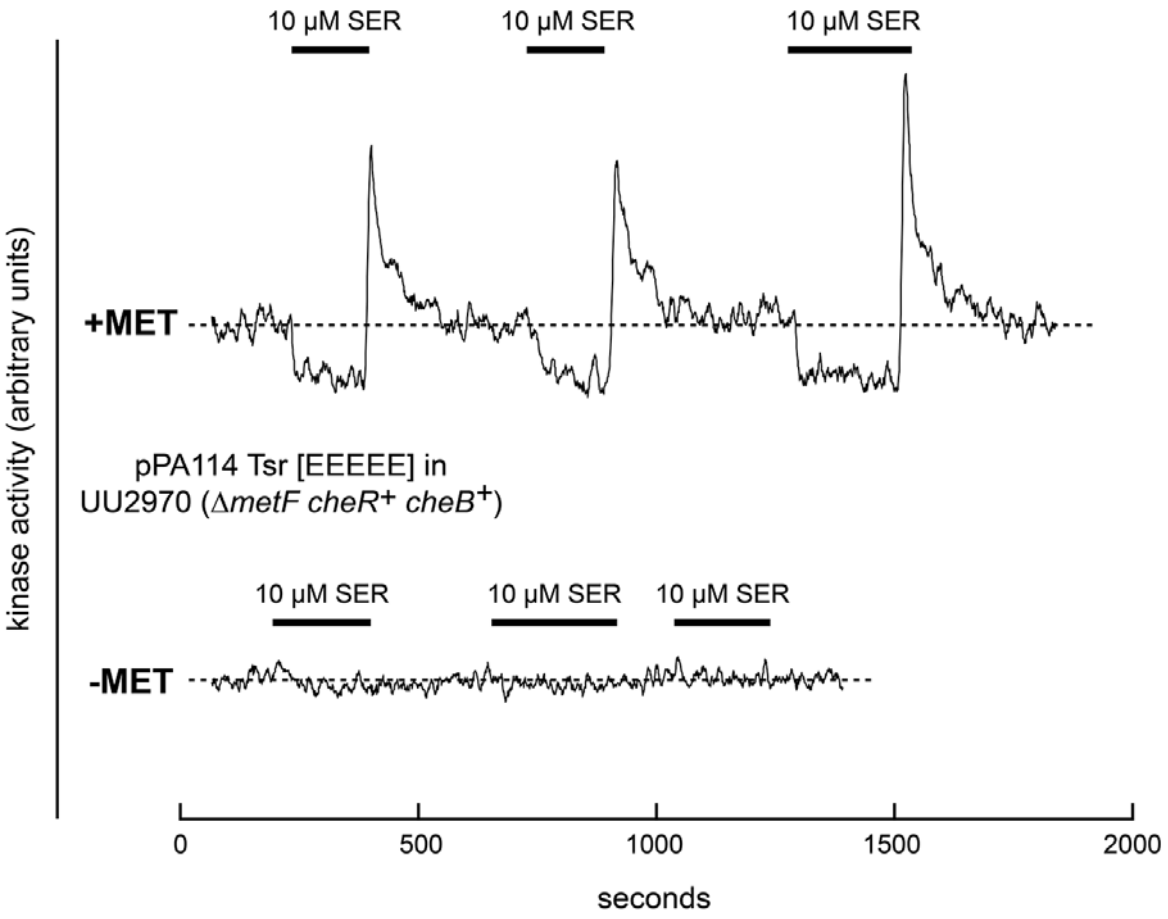

Fig. S6. Validation of the methionine starvation treatment. Cells of adaptation-competent strain UU2970 (R+B+) carried a derivative of plasmid pPA114 expressing Tsr [EEEEE] and a compatible FRET reporter plasmid (pVS88). Data traces from FRET kinase assays of methionine-starved (-MET) and control (+MET) cells follow the ratio of YFP to CFP photon counts in response to application and removal of 10 μM serine stimuli.

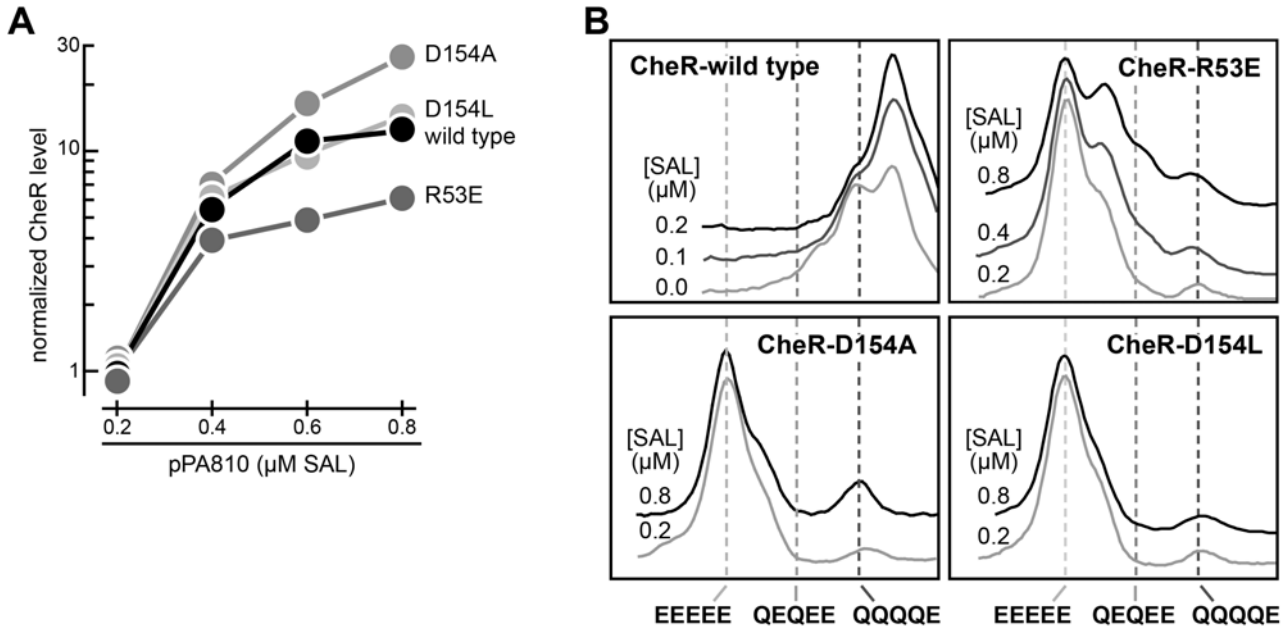

Fig. S7. Expression and functional defects of mutant CheR proteins.

A. Induction profiles of pPA810 derivatives. CheR levels are expressed relative to that for induction with 0.2 μM salicylate. The wild-type CheR data are also presented in the inset of Fig. 4 in the main text.

B. Receptor methylation by wild-type and mutant CheR proteins. Compatible plasmids expressing Tsr [EEEEE] (induced with 100 μM IPTG) and wild type or mutant CheR (induced with various levels of sodium salicylate [SAL]) were expressed in host strain UU2610 (R-B-). Tsr molecules were analyzed by SDS-PAGE and visualized by immunoblotting. Densitometry traces of band profiles were adjusted to the same maximum peak heights but offset vertically to facilitate comparisons between different CheR induction levels. Positions of Tsr [EEEEE], Tsr [QEQEE] and Tsr [QQQQE] reference standards are indicated by broken vertical lines. Small peaks at the QQQQE position in the mutant CheR traces are due to a protein that cross-reacts with anti-Tsr serum.

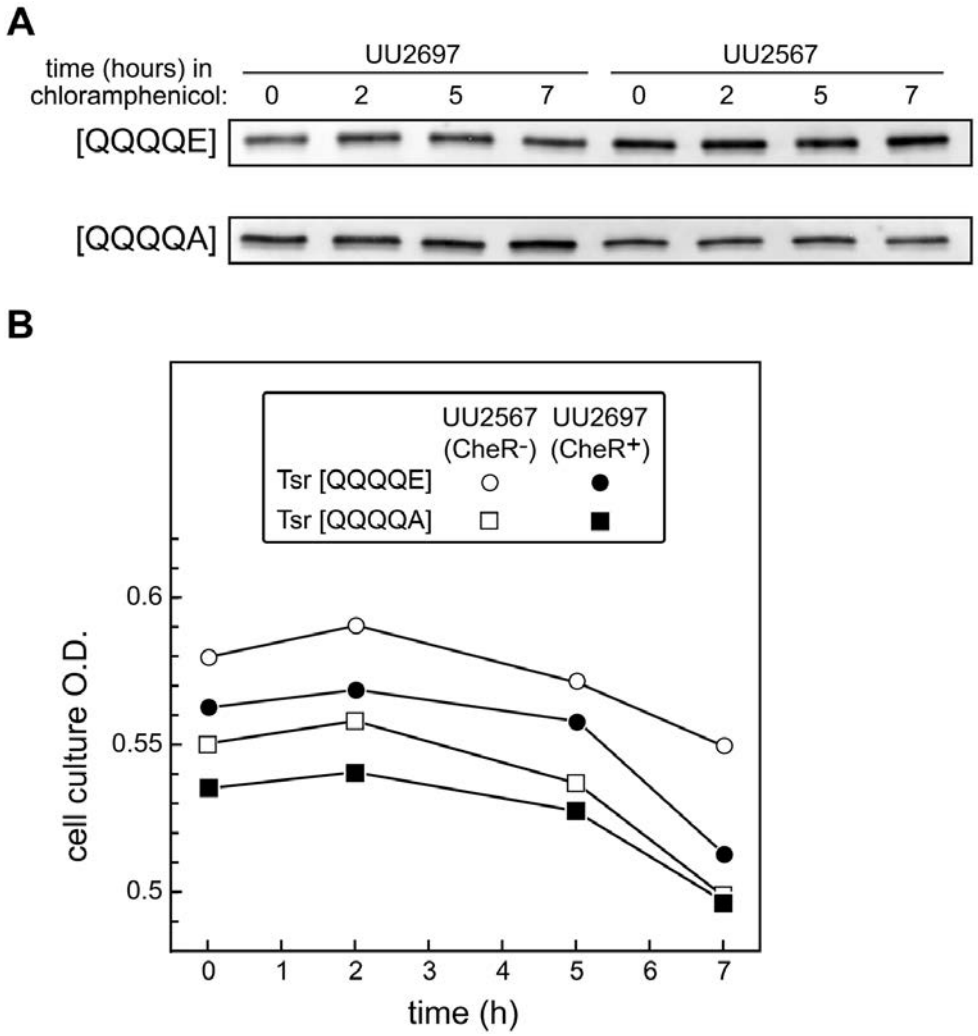

Fig. S8. Tsr levels and cell densities over the timecourse of chloramphenicol treatment .

A. Tsr [QQQQE] and Tsr [QQQQA] in cell samples collected at 0, 2, 5, and 7 hours of chloramphenicol treatment were analyzed by SDS-PAGE and anti-Tsr immunoblotting.

B. Optical density of cell cultures at 0, 2, 5, and 7 hours of chloramphenicol treatment.

Supplemental Tables

Table S1. Strains

strain	relevant genotype	reference
RP4968	*(cheR)Δm58-13*	unpublished lab strain
UU2567	*(tar-cheZ)Δ4211 (tsr)Δ5547 (aer)Δ1 (trg)Δ4543*	(60)
UU2610	*(tar-cheB)Δ4346 (tsr)Δ5547 (aer)Δ1 (trg)Δ4543*	(19)
UU2611	*(tar-cheR)Δ4283 (tsr)Δ5547 (aer)Δ1 (trg)Δ4543*	(19)
UU2612	*(tar-tap)Δ4530 (tsr)Δ5547 (aer)Δ1 (trg)Δ4543*	(19)
UU2632	*(cheB)Δ4345* *(tar-tap)Δ4530 (tsr)Δ5547 (aer)Δ1 (trg)Δ4543*	(19)
UU2697	*(cheY-cheZ)Δ1215 (cheB)Δ4345* *(tar-tap)Δ4530 (tsr)Δ5547 (aer)Δ1 (trg)Δ4543*	(60)
UU2699	*(cheY-cheZ)Δ1215* *(tar-cheR)Δ4283 (tsr)Δ5547 (aer)Δ1 (trg)Δ4543*	(60)
UU2700	*(cheY-cheZ)Δ1215* *(tar-tap)Δ4530 (tsr)Δ5547 (aer)Δ1 (trg)Δ4543*	(60)
UU2902	*prhaBAD::cheZ~cfp pxylAB::cheY~yfp* *(tar-cheZ)Δ4211 (tsr)Δ5547 (aer)Δ1 (trg)Δ4543*	this work
UU2915	*tsr-QQQQE (tar-cheZ)Δ4211 (aer)Δ1 (trg)Δ4543*	this work
UU2961	*cheW-R117D/E121R/F122S* *tsr-QQQQE (tar-cheZ)Δ4211 (aer)Δ1 (trg)Δ4543*	this work
UU2967	*(metF)Δ1297* *tsr-QQQQE (tar-cheZ)Δ4211 (aer)Δ1 (trg)Δ4543*	this work
UU2970	*(metF)Δ1297 (cheY-cheZ)Δ1215* *(tar-tap)Δ4530 (tsr)Δ5547 (aer)Δ1 (trg)Δ4543*	this work

Table S2. Examples of Tsr variants that exhibit CheR-enhanced response sensitivity

Tsr mutant:	potential $+CH_3$ sites in UU2697	response parameters in strain UU2567 ($CheR^-$ $CheB^-$) $K_{1/2}$ (SER)[a] Hill coefficient[a] kinase activity[b]	response parameters in strain UU2697 ($CheR^+$ $CheB^-$) $K_{1/2}$ (SER)[a] Hill coefficient[a] kinase activity[b]
pPA114 derivatives			
[QEQEE][c]	3	17 ± 2.4 μM [4] 18 ± 10 [4] 0.103	51 μM 2.2 0.133
[QQQQE]	1	160 μM 13 0.109	48 ± 6.4 μM [2] 3.9 ± 2.4 [2] 0.080 ± 0.005 [2]
L252F	3	NR NR 0.020 ± 0.004 [2]	1100 2.8 0.126
L263F	3	750 ± 26 μM [3] 6.9 ± 2.1 [3] 0.105	230 μM 3.9 0.082
L225S	3	38 μM 8.1 0.099	6.0 μM 9.7 0.090
E502Q	2	NR NR 0.106	5300 μM 4.1 0.078
pRR53 derivatives			
[QEQEE][c]	3	17 ± 1.1 μM [2] 15 ± 7.5 [2] 0.060	49 ± 6.6 μM [2] 8.5 ± 4.8 [2] 0.126
Q311M	3	NR NR 0.061	450 μM 3.8 0.060
Q311P	3	34 μM 17 0.062	1.2 ± 0.1 μM [2] 1.8 ± 0.1 [2] 0.033

Table S2 (continued)

[NDNDE]	1	48 ± 12 μM [3] 12 ± 5.7 [3] 0.065 ± 0.029 [3]	15 μM 6.8 0.060
[NDNDF]	0	34 ± 5.5 μM [4] 9.5 ± 5.5 [4] 0.066 ± 0.009 [4]	9.0 ± 3.5 μM [2] 8.3 ± 3.8 [2] 0.051 ± 0.025 [2]
[NDNDL]	0	110 ± 12 μM [2] 10 ± 2 [2] 0.069 ± 0.016 [2]	34 ± 15 μM [2] 3.3 ± 1.0 [2] 0.078 ± 0.040 [2]
[NDNDR]	0	1200 ± 20 μM [2] 11 ± 1.1 [2] 0.041 ± 0.011 [2]	120 μM 8.4 0.057
[NDNDV]	0	24 ± 13 μM [3] 9.5 ± 3.0 [3] 0.047 ± 0.013 [3]	7.4 ± 0.8 μM [2] 3.6 ± 0.0 [2] 0.081 ± 0.037 [2]

[a] Values with error ranges represent averages and standard deviations of [n] independent FRET-based dose-response experiments. Values below 10 were rounded to the nearest 0.1; values above 10 were rounded to the nearest 1; values above 100 were rounded to the nearest 10; values above 1000 were rounded to the nearest 100.

[b] Absolute kinase activity was calculated from the FRET response to a saturating SER stimulus or, if no response, to KCN treatment (values in italics) (26, 60).

[c] Although Tsr wild-type [QEQEE] shows a higher $K_{1/2}$ in UU2697 (R+B-) than in UU2567 (R-B-), that response appears to be a compromise between the ON-shifting effect of a higher methylation state and the OFF-shifting effect of CheR enhancement. Note that in UU2697 the Tsr [QEQEE] $K_{1/2}$ is comparable to the Tsr [QQQQE] $K_{1/2}$.

NR: no response to 10 mM serine.

Table S3. Effect of elevated CheR expression on response enhancement.

			$K_{1/2}$ (SER)[a] Hill coefficient[a] kinase activity[b]		
		Tsr:	[QQQQA]	[QQQQE]	[QQQQE]
CheR plasmid	relative CheR level	host:	UU2902	UU2902	UU2915
pKG116 (null)	0		170 μM 9.7 0.040	180 ± 16 μM [2] 7.6 ± 6.2 [2] 0.019	170 μM 12 0.062
pPA810 (*cheR*$^+$) [SAL][c]					
0 μM	1.5		14 μM 5.5 0.027	21 μM 4.3 0.024	20 μM 11 0.052
0.1 μM	5.3		11 μM 13 0.054	14 μM 5.3 0.021	19 μM 9.2 0.041
0.2 μM	35		6.2 μM 4.3 0.008	13 μM 9.1 0.014	16 μM 17 0.044
0.4 μM	106		4.3 μM 4.9 0.039	7.1 μM 3.3 0.024	11 μM 44 0.056
0.6 μM	248		2.4 μM 3.0 0.058	8.6 μM 11 0.022	9.9 μM 16 0.083
0.8 μM	339		1.4 μM 3.4 0.040	5.8 μM 11 0.020	12 μM 12 0.068

[a] Values with error ranges represent averages and standard deviations of [n] independent FRET-based dose-response experiments. Values below 10 were rounded to the nearest 0.1; values above 10 were rounded to the nearest 1; values above 100 were rounded to the nearest 10.

[b] Absolute kinase activity was calculated from the FRET response to a saturating SER stimulus.

[c] Concentration of sodium salicylate inducer.

Table S4. Response parameters of Tsr [NDNDX] variants ± NWETF in four hosts

Tsr mutant (in pRR53)	host:	$K_{1/2}$ (SER)[a] / Hill coefficient[a] / kinase activity[b]			
		UU2567 ($CheR^-$ $CheB^-$)	UU2697 ($CheR^+$ $CheB^-$)	UU2699 ($CheR^-$ $CheB^+$)	UU2700 ($CheR^+$ $CheB^+$)
[QEQEE] (+NWETF)		17 ± 1.1 μM [2] 15 ± 7.5 [2] 0.060	49 ± 6.6 μM [2] 8.5 ± 4.8 [2] 0.126	NR NR *0.005*	0.4 ± 0.1 μM [2] 2.4 ± 0.2 [2] 0.029
[QEQEE] ΔNWETF		32 μM 11 0.043	35 μM 14 0.039	0.9 μM 4.2 0.007	1.0 μM 3.3 0.007
[NDNDF] (+NWETF)		34 ± 5.5 μM [4] 9.5 ± 5.5 [4] 0.066 ± 0.009 [4]	9.0 ± 3.5 μM [2] 8.2 ± 3.8 [2] 0.051 ± 0.025 [2]	38 ± 2.5 μM [2] 6.3 ± 0.2 [2] 0.070	18 ± 2.4 μM [2] 6.7 ± 0.2 [2] 0.050 ± 0.017 [2]
[NDNDF] ΔNWETF		32 μM 16 0.044	23 μM 8.6 0.029	25 μM 9.2 0.060	24 μM 12 0.055
[NDNDL] (+NWETF)		110 ± 12 μM [2] 10 ± 2 [2] 0.069 ± 0.016 [2]	34 ± 15 μM [2] 3.3 ± 1.0 [2] 0.078 ± 0.040 [2]	110 ± 28 μM [2] 1.9 ± 0.3 [2] 0.078 ± 0.015 [2]	31 μM 5.2 0.050
[NDNDL] ΔNWETF		97 μM 6.8 0.045	108 μM 5.6 0.055	130 μM 7.0 0.038	94 μM 13 0.077
[NDNDR] (+NWETF)		1200 ± 20 μM [2] 11 ± 1.1 [2] 0.041 ± 0.011 [2]	118 μM 8.4 0.057	2090 μM 2.2 0.051	73 ± 10 μM [2] 5.1 ± 3.0 [2] 0.072 ± 0.013 [2]
[NDNDR] ΔNWETF		2800 μM 2.7 0.096 ± 0.028 [2]	1600 μM 2.9 0.025	2000 μM 5.5 0.028	1500 μM 3.5 0.046 ± 0.029 [2]
[NDNDV] (+NWETF)		24 ± 13 μM [3] 9.5 ± 3.0 [3] 0.047 ± 0.013 [3]	7.4 ± 0.8 μM [2] 3.6 ± 0.1 [2] 0.081 ± 0.037 [2]	28 ± 8.3 μM [2] 5.3 ± 1.6 [2] 0.026	18 μM 6.6 0.067
[NDNDV] ΔNWETF		23 ± 12 μM [2] 8.9 ± 2.4 [2] 0.073 ± 0.003 [2]	38 ± 4.3 μM [2] 17 ± 2.6 [2] 0.064 ± 0.001 [2]	35 ± 6.1 μM [2] 20 ± 1.5 [2] 0.074	20 ± 8.4 μM [2] 8.3 ± 1.7 [2] 0.045

[a] Values with error ranges represent averages and standard deviations of [n] independent FRET-based dose-response experiments. Values below 10 were rounded to the nearest 0.1; values above 10 were rounded to the nearest 1; values above 100 were rounded to the nearest 10; values above 1000 were rounded to the nearest 100.

[b] Absolute kinase activity was calculated from the FRET response to a saturating SER stimulus or, if no response, to KCN treatment (italicized values).

NR: no detectable response to 10 mM serine.

Table S5. Effect of CheR lesions and NWETF ablation on response enhancement.

		$K_{1/2}$ (SER)[a] / Hill coefficient[a] / kinase activity[b]			
	Tsr:	[QQQQE] ΔNWETF	[QQQQE]	[QQQQE]	[QQQQE]
CheR plasmid	host:	UU2902	UU2902	UU2902	UU2902
pKG116 (null)		240 μM 6.7 0.028	<----------	180 ± 16 μM [2] 7.6 ± 6.2 [2] 0.019	---------->
pPA810 derivative: [Na salicylate]		wild-type CheR	CheR-D154A	CheR-D154L	CheR-R53E
0 μM		270 μM 6.1 0.038	nd	nd	nd
0.4 μM		nd	160 μM 7.9 0.026	170 μM 4.2 0.014	120 μM 5.6 0.017
0.8 μM		48 μM 2.9 0.022	140 μM 3.8 0.015	110 μM 3.5 0.008	100 μM 5.6 0.041

[a] Values with error ranges represent averages and standard deviations of [n] independent FRET experiments. Values below 10 were rounded to the nearest 0.1; values above 10 were rounded to the nearest 1; values above 100 were rounded to the nearest 10.

[b] Absolute kinase activity was calculated from the FRET response to a saturating SER stimulus.

nd: not determined.

Table S6. Effect of methionine starvation on response enhancement.

		$K_{1/2}$ (μM)[a] / Hill coefficient[a] / kinase activity[b]	
	Tsr:	[QQQQE]	[QQQQE]
CheR plasmid	host:	UU2967 [- MET]	UU2967 [+ MET]
pKG116 (null)		170 μM 17 0.046	170 μM 16 0.060
pPA810 (*cheR*$^+$): [SAL][c]			
0 μM		14 μM 14 0.048	17 μM 17 0.047
0.1 μM		12 μM 25 0.047	16 μM 40 0.033
0.2 μM		9.9 μM 13 0.048	11 μM 14 0.057
0.4 μM		9.5 μM 13 0.070	10 μM 51 0.042
0.6 μM		8.7 μM 9.6 0.042	6.2 μM 6.4 0.043
0.8 μM		7.6 μM 9.4 0.047	7.6 μM 8.1 0.050

[a] Values below 10 were rounded to the nearest 0.1; values above 10 were rounded to the nearest 1; values above 100 were rounded to the nearest 10.

[b] Absolute kinase activity was calculated from the FRET response to a saturating SER stimulus.

[c] Concentration of sodium salicylate inducer.

nd: not determined.

Table S7. CheR response enhancement in chloramphenicol-treated cells.

	$K_{1/2}$ (μM)[a] / Hill coefficient[a]			
Tsr:	[QQQQE]		[QQQQA]	
host:	UU2567 (R-B-)	UU2697 (R+B-)	UU2567 (R-B-)	UU2697 (R+B-)
hours in chloramphenicol				
0	170 μM 17	51 μM 5.3	160 ± 2 μM [2] 20 ± 2.1 [2]	27.5 ± 5 μM [2] 8.8 ± 7.3 [2]
2	170 μM 17	39 μM 5.2	160 ± 14 μM [2] 16 ± 2.8 [2]	18 μM 6.8
5	170 μM 14	30 μM 5.9	155 ± 7.1 μM [2] 15.5 ± 5 [2]	13 ± 0 μM [2] 8.7 ± 1.8 [2]
7	180 μM 17	23 μM 5.3	168 μM 13	12 μM 9.3

[a] Values with error ranges represent averages and standard deviations of [n] independent FRET experiments. Values below 10 were rounded to the nearest 0.1; values above 10 were rounded to the nearest 1; values above 100 were rounded to the nearest 10.